Ministry for Primary Industries
Manatū Ahu Matua

Abundance and Distribution of WCSI Hector's dolphin

New Zealand Aquatic Environment and Biodiversity Report No. 168.

D.I. MacKenzie,
D.M. Clement

ISSN 1179-6480 (online)
ISBN 978-1-77665-236-5 (online)

April 2016

New Zealand Government

Growing and Protecting New Zealand

Requests for further copies should be directed to:

Publications Logistics Officer
Ministry for Primary Industries
PO Box 2526
WELLINGTON 6140

Email: brand@mpi.govt.nz
Telephone: 0800 00 83 33
Facsimile: 04-894 0300

This publication is also available on the Ministry for Primary Industries websites at:
http://www.mpi.govt.nz/news-resources/publications.aspx
http://fs.fish.govt.nz go to Document library/Research reports

TABLE OF CONTENTS

EXECUTIVE SUMMARY

MacKenzie, D.I.; Clement, D.M. (2016). Abundance and distribution of WCSI Hector's dolphin. ***New Zealand Aquatic Environment and Biodiversity Report No. 168.*** **67 p + supplemental material.**

The Ministry for Primary Industries and the Department of Conservation are currently reviewing the Hector's dolphin Threat Management Plan. For this review, up-to-date abundance and distribution estimates of Hector's dolphin are required. A survey programme was specifically designed for sampling the WCSI population using two separate aerial surveys over summer 2014/2015 and winter 2015. The WCSI surveys constitute the last abundance estimate of the three regional South Island Hector's dolphin sub-populations; following on from the east and north coast (ECSI) aerial surveys in 2013 (MacKenzie & Clement 2014) and south coast (SCSI) aerial surveys in 2010 (Clement et al. 2011). This report summarises the results from the recently completed WCSI surveys.

The WCSI survey area (about 26 333 km^2 between Farewell Spit and Milford Sound) was stratified into six coastal sections, which were further divided into offshore substrata of 0–4 nmi (inner), 4–12 nmi (middle) and 12–20 nmi (outer). This design was expected to encompass the offshore limits of Hector's dolphin distribution along the South Island's west coast. Double observer, line-transect methodology was used with transect lines orientated in the offshore direction and spaced parallel at equal intervals (according to strata-specific effort allocation) using systematic-random line placement.

WCSI abundance was estimated using an extension of mark-recapture distance sampling (MRDS) techniques that accounts for differing field of views between observer positions in the plane; similar to the approach developed for the ECSI survey (MacKenzie & Clement 2016). These methods also allow for a lack of independence between the observer detections. Availability bias is a fundamentally important component for obtaining a reliable estimate of total abundance. As in the ECSI survey, we utilise two availability methods; helicopter observations of dive cycles and circle-back redetection.

These aerial surveys constitute the only abundance study to date with substantial effort in offshore regions (more than 4 nmi from the coast) for Hector's dolphin along the entire west coastal waters of the South Island. Summer sightings results consisted of 250 dolphin groups (115 of which were seen by two observers) sighted within 0.3 km either side of the plane along 4001 km of transect lines. In winter, 272 dolphin groups (115 of which were seen by two observers) were sighted within 0.3 km either side of the plane along 4307 km of transect lines. Hector's dolphins were observed as far offshore as 12 km (6.5 nmi) and 17.7 km (9.5 nmi) in summer and winter, and in waters as deep as 160 m and 200 m, respectively. However, the majority of animals in both seasons occurred close to shore (less than 3 nmi) and within relatively shallow depths (less than 40 m).

Regional variation in dive cycle data was similar in both survey periods with slightly lower surface availability off the Okarito Lagoon region. Availability estimated from the circle-back data exhibited less regional variation than dive-profiles, although both the effects of region and offshore (0–4 nmi or 4–20 nmi) factors were incorporated into model average estimates of circle-back availability.

The WCSI Hector's dolphin summer abundance was estimated to be 5490 (CV: 26%; 95% CI: 3319–9079) and 5802 (CV: 21%, 95% CI: 3879–8679) in winter. These estimates were obtained by averaging the four sets of results for each season; from two different data sets using different truncation distances and two methods of estimating availability (dive cycle and circle-backs). These estimates are very similar to the previous 2000/2001 WCSI estimate of 5388 Hector's dolphins (CV: 21%; 95% CI: 3613–8034), even after accounting for differences in offshore survey areas.

Following a reanalysis of the ECSI and SCSI survey data, our estimate for the total Hector's population around the South Island (excluding sounds and harbours) is 14 849 (CV: 11%, 95% CI

11 923–18 492). This estimate is approximately double the previous estimate from surveys conducted in the late 1990s – early 2000s (7300; 95% CI 5303–9966), with the difference primarily due to a much larger estimated population along ECSI, distributed much further offshore than previously thought. Densities are similar along ECSI and WCSI. This new estimate has implications regarding the conservation, potential fisheries-related impact and our general understanding of the species.

1. INTRODUCTION

Hector's dolphin, *Cephalorhynchus hectori hectori*, is only found within New Zealand waters and is currently listed as *Nationally Endangered* by the NZ threat classification scheme (Baker et al. 2010) and considered *Endangered* by the IUCN since 2000 (Reeves et al. 2008). From a series of surveys conducted from 1997–2001, the population of this species around the South Island has been estimated at approximately 7300 animals (95% 5303–9966; Slooten et al. 2004).

MPI and DOC have agreed to undertake a review of the Hector's Dolphin Threat Management Plan in 2018 as this species' coastal distribution significantly overlaps with inshore setnet and trawl fisheries (DOC & MFish 2007). As part of this process, decision-makers must take into account sections 8, 9, and 15 of the Fisheries Act 1996, which include guidance to avoid, remedy or mitigate any adverse effects of fishing on the aquatic environment, including the effects of fishing related mortality on protected species. For this review, an up-to-date abundance estimate of Hector's dolphin is required as the previous estimate is now too old for management purposes and more recent research demonstrates that this species ranges further offshore than past abundance surveys have sampled (e.g. DuFresne & Mattlin 2009, Rayment et al. 2010a).

1.1 Background

The South Island population of Hector's dolphin is clumped, geographically and genetically, into three fairly distinct sub-populations (Dawson & Slooten 1988, Pichler et al. 1998, Hamner et al. 2012). Based on previous estimates (Slooten et al. 2004), the majority of dolphins (about 3600 to 8000) were thought to occur along the West Coast (WCSI; between Farewell Spit and Milford Sound) with the remainder found along the East Coast (ESCI; from Farewell Spit to Nugget Point) and South Coast (SCSI; from Nugget Point to Long Point).

This abundance estimate is based on a series of four surveys, three undertaken by boat and one by airplane, over four consecutive summer seasons between 1997/1998 and 2000/2001. All four surveys were based on line-transect sampling methods and targeted the inshore waters between the coastline and four nautical miles (nmi) offshore. Sparse sampling effort was allocated to more offshore regions as previous research (Dawson & Slooten 1988) suggested few dolphins occurred beyond four nmi. As a result, abundance was not estimated for more offshore waters (Dawson et al. 2004, Slooten et al. 2004).

In 2008, the Ministry of Fisheries (now MPI) and Department of Conservation (DOC) released a draft Hector's and Maui's Dolphin Threat Management Plan (TMP). This management document highlighted fishing-related mortalities as one of the main human-induced, yet highly uncertain, threats to this species. To mitigate such effects, the TMP established a range of fisheries prohibited zones and several non-fisheries protective measures throughout the three sub-populations based on the above abundance estimates and all available data (DOC & MFish 2007). These measures focused on the waters out to four nmi where the majority of dolphins occur and overlap with both commercial and recreational setnet fisheries and inshore trawl fisheries.

Since the abundance surveys were completed and the TMP measures implemented, additional aerial-based studies have been undertaken within several localised regions around the South Island (i.e. DuFresne & Mattlin 2009, DuFresne et al. 2010, Rayment et al. 2010a, 2010b, Clement et al. 2011). There are several advantages to using aerial platforms for research on

Hector's dolphins. The biggest advantages include being able to synoptically sample a large study area in much shorter time periods than boat platforms, which minimises the effect of any directional or seasonal movement while also eliciting little to no responsive behaviours from the dolphins (Slooten et al. 2004).

All of these studies found Hector's dolphin regularly occurring past four nmi and some much further offshore than previously thought this species might normally occur (e.g. 16 nmi DuFresne & Mattlin 2009; 18 nmi Rayment et al. 2010a). In addition, recent abundance surveys along the east and north coasts (MacKenzie & Clement 2014) indicated much larger regional populations of Hector's dolphins present over summer than the previous abundance survey estimated (Slooten et al. 2004). These findings suggest that the 1997–2001 abundance survey may have missed a proportion of dolphins from these offshore regions and that the overall population of Hector's dolphin is likely to be larger than previously estimated.

1.2 Scope

The Cawthron Institute (Cawthron), in conjunction with Proteus Wildlife Research Consultants, were contracted by MPI to conduct two aerial surveys along the WCSI in summer 2014/2015 and winter 2015. The resulting survey programme was designed specifically for the WCSI population and based on previous aerial methods for this species (MacKenzie & Clement 2014, 2016). This study constitutes the last abundance estimate of the three regional Hector's dolphin sub-populations; following on from the ECSI aerial surveys in 2013 (MacKenzie & Clement 2014) and SCSI aerial surveys in 2010 (Clement et al. 2011).

The previous design work for the ECSI survey (under contract PRO2009/01B) also identified inconsistencies in how sightings of dolphin groups within the observer overlap zone have been incorporated in the detection function analysis when estimating Hector's dolphin abundance by different researchers. As a result, the earlier SCSI aerial surveys (Clement et al. 2011) were reanalysed using the same general approach to the detection function modelling as that used for the ECSI and WCSI analyses in order to calculate a combined South Island population estimate for Hector's dolphins. The specific scope of this programme is outlined as follows.

Overall Objective:

To estimate the abundance and distribution of the West Coast South Island population of Hector's dolphins and compile the most recent abundance and distribution estimates for all Hector's dolphins populations around the South Island to enable assessments of population status, trends and the effects of fishing-related mortality on all populations.

Specific Objectives:

1. To develop and refine design and analysis methods for summer and winter aerial surveys for Hector's dolphins along the WCSI consistent with the recent ECSI surveys.
2. To estimate the abundance of Hector's dolphins along the WCSI in summer 2014/2015 applying an agreed aerial survey methodology.
3. To estimate the distribution of Hector's dolphins along the WCSI in summer 2014/2015 applying an agreed aerial survey methodology.
4. To estimate the abundance of Hector's dolphins along the WCSI in winter 2015 applying an agreed aerial survey methodology.

5. To estimate the distribution of Hector's dolphins along the WCSI in winter 2015 applying an agreed aerial survey methodology.
6. To compile and reanalyse, where necessary, recent survey data to estimate Hector's dolphin abundance and distribution throughout the South Island applying an agreed approach to estimating the detection function.

2. METHODS

For Objectives 1–5, the survey programme was based on the general aerial survey design outlined in MacKenzie et al. (2012) as they have been previous applied and refined on the ECSI survey (MacKenzie & Clement 2014). Detailed discussions of the survey protocols and methods are provided in MacKenzie & Clement (2014) and a brief summary as they have been applied to the WCSI survey is given below.

Related to Objective 6, the aerial survey and data collection protocols for the SCSI surveys have been previously described by Clement et al. (2011). The general analysis approach used for the SCSI reanalysis is the same as that used for WCSI abundance estimates. Section A in the Supplemental Material (SM) gives a brief review of the survey design along with details of the detection function analysis that are specific to the SCSI data set. For consistency, the ECSI data were also reanalysed for Objective 6 using the symmetric parameterisation of the detection function modelling that was used for the WCSI surveys (see MacKenzie & Clement 2016).

2.1 WCSI survey design and effort

The 26 333 km^2 of the WCSI survey area was stratified into six coastal sections and each divided into three offshore substrata of 0–4 nmi (inner), 4–12 nmi (middle) and 12–20 nmi (outer - see Table 1), as agreed upon at the August 2014 AEWG meeting. This design was expected to encompass the distributional limits of Hector's dolphin along the west coast.

The summer survey of all continuous transect lines (252 lines, 4001 km) was carried out between 26 January and 1 March 2015. Note that the offshore stratification subdivides many of the continuous transects, hence there was a total of 360 transect lines for the purpose of the analysis (Figure 1; i.e. one continuous transect line may be considered as three lines for analysis purposes if it spans across all three offshore substrata). More intensive sampling was allocated within known high-density regions (e.g. Westport and Okarito Lagoon; Table 1). Less intensive sampling was carried out in suspected low-density strata, although effort was still greater than what would be considered optimal for estimating abundance (MacKenzie et al. 2012) in recognition that little survey work has been conducted in those areas and for the dual survey objectives of estimating abundance and distribution.

The survey design was further optimised for winter sampling by reallocating sampling effort to and from particular coastal sections and offshore substrata based on summer sighting results. Effort changes included reducing effort in the furthest offshore strata (12–20 nmi) and within the inner substrata off Whanganui Inlet (previously over-sampled as the summer survey suggested that local abundance was a smaller proportion of WCSI population then anticipated; Table 1; Figure 1). Survey effort was then reallocated and increased off Greymouth's inner substrata (0–4 nmi) and both Hector's and Okarito's middle substrata (4–12 nmi) as summer results suggested these areas were possibly under-sampled over summer (Table 1; Figure 1). The winter survey sampled 264 continuous transect lines (4307 km) between 4 July and 1 August 2015 for a total of 396 lines for analysis.

Table 1: Summer and winter survey line spacing with estimated and achieved levels of effort in each stratum.

		SUMMER			WINTER		
Coastal Section	**Offshore Stratum**	**Line Spacing (km)**	**Estimated Length of Transects (km)**	**Achieved Length of Transects (km)**	**Line Spacing (km)**	**Estimated Length of Transects (km)**	**Achieved Length of Transects (km)**
Whanganui Inlet	Inner	7.4	92	91	11.1	59	59
	Middle	11.1	130	130	11.1	128	128
	Outer	11.1	146	145	22.2	70	70
Hector	Inner	1.85	660	647	1.85	659	647
	Middle	7.4	330	330	3.7	660	660
	Outer	11.1	222	221	22.2	104	104
Greymouth	Inner	3.7	257	253	1.85	517	510
	Middle	11.1	162	162	11.1	165	164
	Outer	11.1	151	151	22.2	78	78
Okarito Lagoon	Inner	1.85	614	606	1.85	614	605
	Middle	7.4	297	297	3.7	591	590
	Outer	11.1	198	198	22.2	108	108
Jackson Bay	Inner	3.7	195	191	3.7	195	191
	Middle	11.1	131	131	11.1	115	115
	Outer	11.1	128	128	22.2	61	61
Milford Sound	Inner	7.4	98	95	7.4	97	95
	Middle	11.1	107	107	22.2	62	62
	Outer	11.1	117	117	22.2	61	61
Total			**4035**	**4001**		**4343**	**4307**

A)

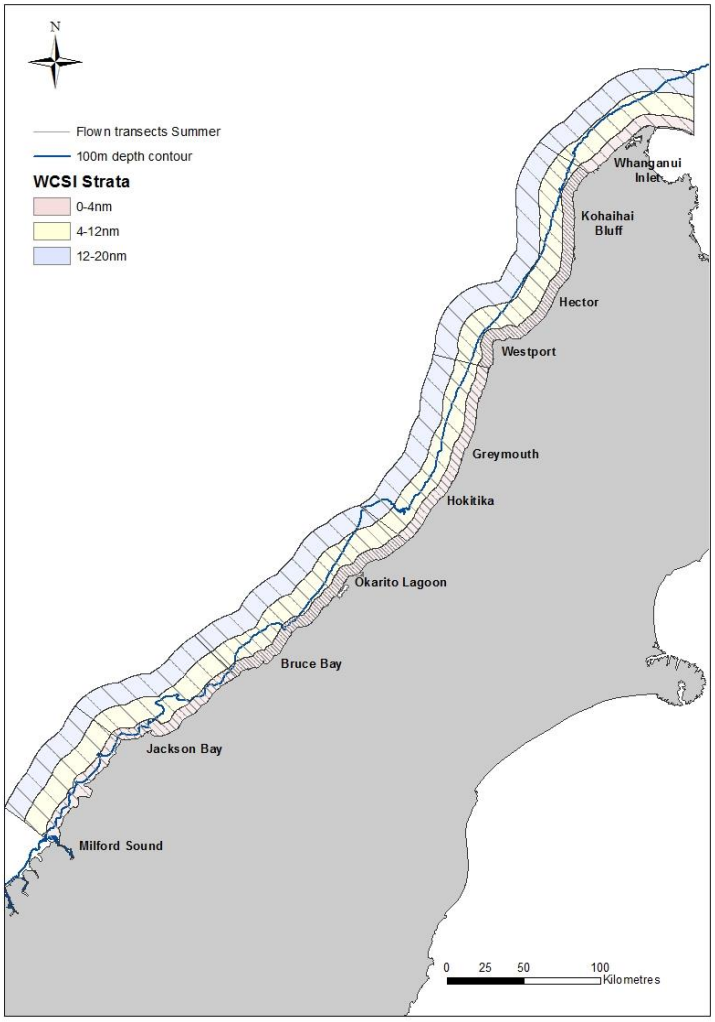

B)

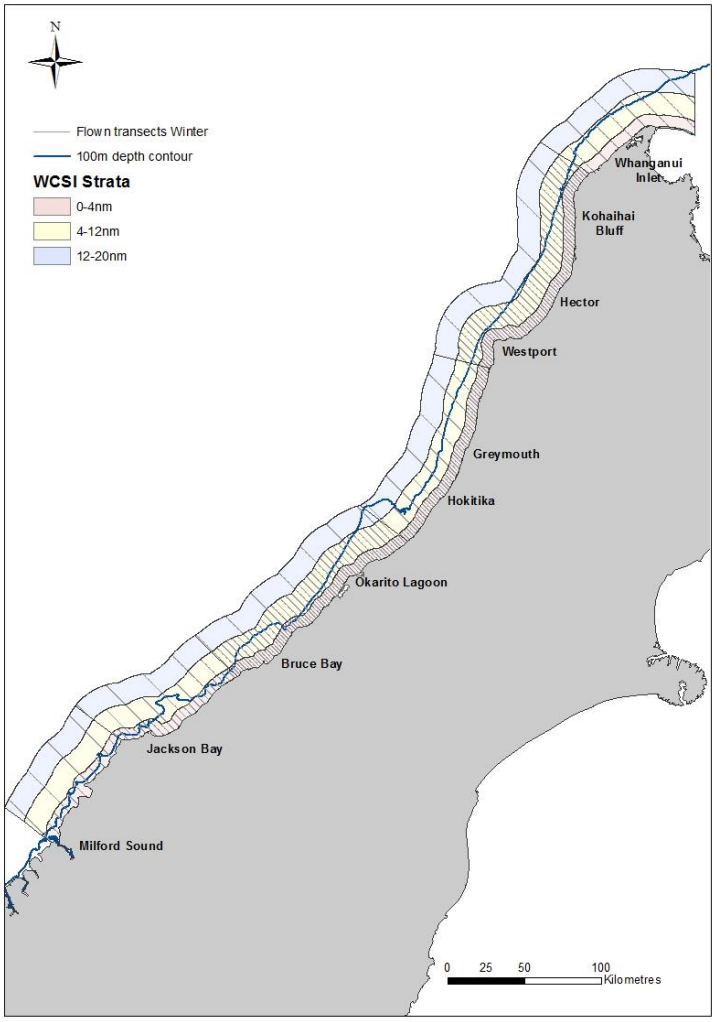

Figure 1: A) WCSI summer survey transects flown between 26 January and 1 March 2015. B) WCSI winter survey transects flown between 4 July and 1 August 2015.

2.2 WCSI survey platform and protocol

The same high-wing, seven-seater Cessna 207 aircraft was used as in the ECSI 2013 surveys. This plane allows two observers to independently search for Hector's dolphins, one on each side of the aircraft. Rear bubble windows permitted observers in the back seats to see directly underneath the plane while surveying. Transects were surveyed at an altitude of 152.4 metres (500 feet) at a speed of approximately 100 knots (185.2 km/h). Surveys were only undertaken in suitable conditions; Beaufort sea state (Beaufort 3 or less), glare intensity (1 to 3 with no fog or obstructive clouds), and good light conditions (one hour after sunrise and before sunset). Additional sighting condition information collected included; percent glare (recorded as the proportion of the field of view obscured), glare direction, water colour (categorised as blue, blue-green, green or brown), and swell height.

Front observers' search zone was between the downward angles of 20°–70°. For the rear observers using the bubble window the search zone was 25°–90°. Each observer recorded downward angle and time (to the second) of each observation into individual dictaphones, as well as other relevant sighting information (e.g. group size, presence of calves, sighting conditions). To minimise the chance of one observer visually cueing off the other, black sheets of fabric were hung between the two seats on each side of the plane. Observers were rotated amongst all positions in the aircraft such that each person spent approximately the same amount of time in each position.

A team of five observers was trained for both the summer and winter survey to ensure consistency across survey results while keeping observers fresh and attentive, and avoiding costly delays due to observer sickness or other unforeseen circumstances. Three of these observers were used across both survey seasons; and in each survey, at least two of the observers had previously taking part in the ECSI Hector's dolphin surveys. Two observers (Ob4 and Ob10) were not available for the winter survey and were replaced by a former observer (Ob2) and a new observer (Ob11). However, the new observer (Ob11) had to leave the project during winter training for personal reasons.

As observers had various levels of marine mammal observing and aerial survey experience, extensive pre-survey training was conducted around Westport (a high-density region for Hector's dolphins) both seasons; 20–26 January 2015 and 17–25 June 2015. Training flights helped confirm the size of the fields of view for observers, ensured that observers were skilled in the field protocols and recording requirements, and helped to re-familiarise the pilot with the survey design, protocols and communication with observers.

Approximately 31 hours of summer (about 18 flights) and 34 hours of winter (about 15 flights) training flights were completed, with individual observer training hours varying between 21.2 and 29.2 hrs both season (Table 2). Summer observers flew 132 transects and made 399 training sightings, and winter observers recorded 234 sightings across 168 transects. All newly trained observers recorded 37 or more sightings each (Table 2, Figure 2) before surveying commenced, well over the recommended 20 sightings minimum (Dawson et al. 2008).

To gauge observer performance, each observer's training sightings were compared against more experienced observers when on the same side of the plane (i.e. number of duplicate sightings versus number of experienced observer sightings within shared viewing zone only).

By the end of both training periods, the detection rates of observers ranged between 71 and 92% (Table 2) of that of the more experienced observers.

Training data were used for training purposes only and not included in any further analyses.

Table 2: Observer statistics from training flights off Westport and Okarito Lagoon (for Ob10 summer only). Note – the numbering of observers is continued from the ECSI surveys (MacKenzie & Clement 2014).

		Ob1	Ob2	Ob4	Ob8	Ob9	Ob10	Ob11
Summer	**Flying Hours**	22.33	-	21.15	25.47	25.47	22.40	-
	On-effort Sightings	78	-	78	62	75	75	-
	Training Detection Rate	89%	-	80%	92%	88%	71%*	-
Winter	**Flying Hours**	21.52	25.60	-	23.97	22.78	-	29.18
	On-effort Sightings	32	49	-	59	47	-	37
	Training Detection Rate	83%	75%	-	79%	79%	-	75%

* compared to the rear seat observer during survey flights

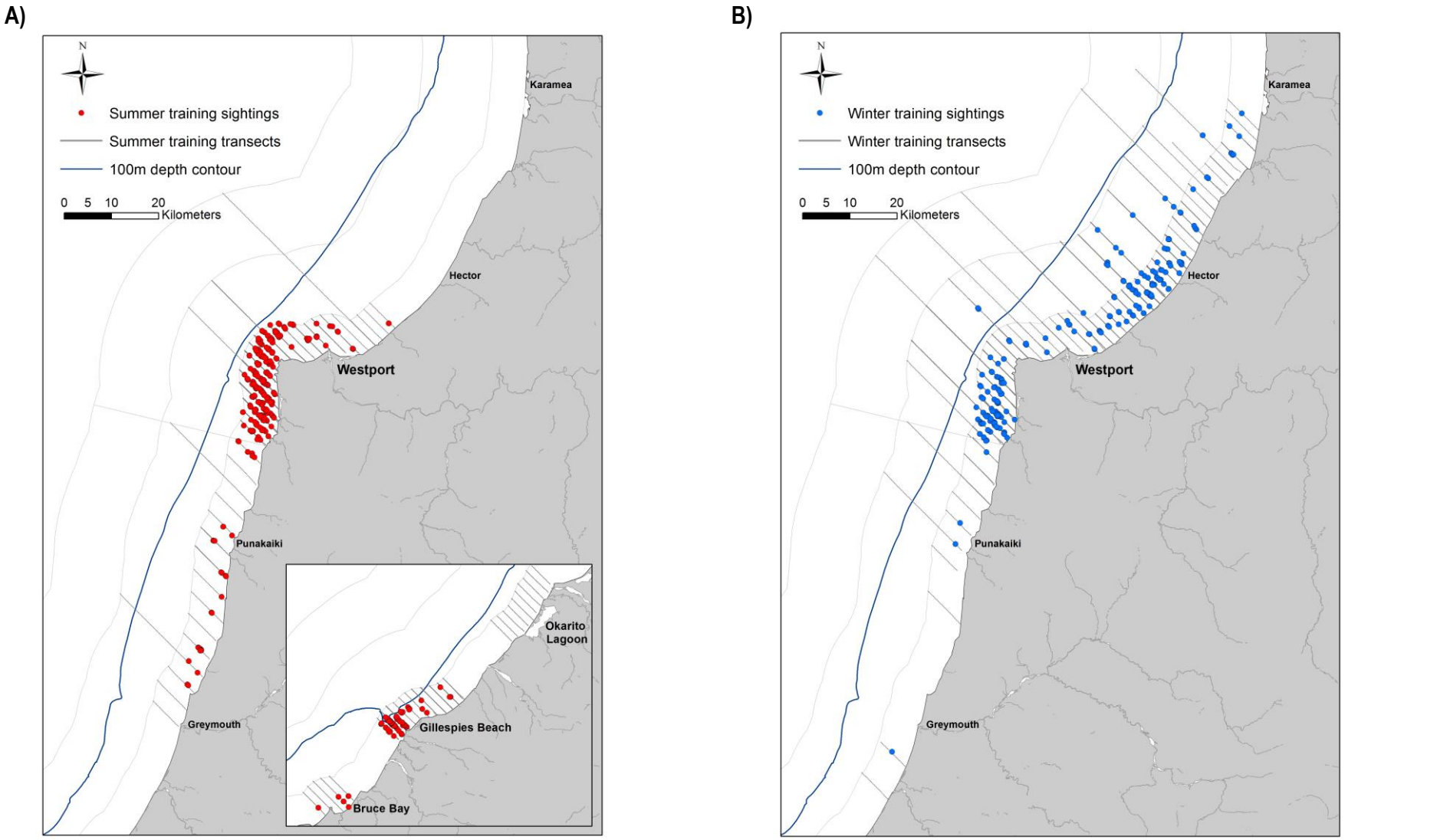

Figure 2: The locations of Hector's dolphin sightings and transects flown during observer training off Westport and Okarito Lagoon (inset) for A) summer: 20–26 January 2015 and B) winter: 17–25 June 2015.

2.3 Abundance Analyses

Data Selection

Any sightings that were data deficient (e.g. angle not measured, seconds not heard, uncertain about species' identification) were removed prior to analysis (Table 3). A right truncation distance of 0.3 km (27 degrees) was used for both front and rear observer positions. This is smaller than the truncation distance used in other aerial surveys for Hector's dolphin (0.33 km - Slooten et al. 2004; 0.337 km – Clement et al. 2011), but consistent with the truncation distance used on ECSI (MacKenzie & Clement 2014). A left-truncation distance of 0.071 km (65 degrees) was used for the front observer position as not all observers could consistently survey to 70 degrees due to their height. Any angles recorded at greater than 90 degrees from the rear observer position were presumed to be 90 degrees. A subset of the data was also analysed where a left truncation distance of 0.071 km was applied to both front and rear observer data as a comparison with the results obtained from the full analysis

Table 3: The numbers of sightings removed through data verification prior to inclusion in abundance or distribution analyses. Sightings were initially removed due to either uncertainty around species identification or missed information about the exact time or angle of the sighting. Additional sightings were removed as part of the left and right truncation process. Final sightings numbers represent those sightings used in the final full analyses. The numbers in brackets list the percentage of the total raw sightings that each verification step represents.

	Raw sighting #	Uncertain about identification	Missed angle/time	Truncated ^	Final Sighting #
Summer	270	3 (1%)	3 (1%)	14 (5%)	**250**
Winter	283	2 (<1%)	0	9 (3%)	**272**

^ Sightings were left truncated at 0.071 km for the front observer position, and right truncated at 0.300 km for both observer positions.

Duplicate sightings were those in which the same group of animals was recorded by both the front and rear observer (on the same side of the plane). Duplicates were manually identified by comparing three different sighting variables; sighting time (within ± 5 seconds), sighting angle (within ± 5 degrees) and group size (± 1 individual), in line with criteria from the previous ECSI and other Hector's dolphin aerial surveys (e.g. DuFresne & Mattlin 2009, Clement et al. 2011), as well as any distinguishing comments recorded by observers (e.g. mother/calf pair, birds nearby).

Duplicate sightings were retained in the final database as a single sighting in which the average angle was used to calculate distance from the trackline, and where the recorded groups sizes differed, the larger value was retained (i.e. 13% of summer and 14% of winter duplicates, respectively). As observers were instructed to record the minimum group size they were certain of rather than approximating group size, the larger value was used as it was believed that undercounting of a group would be more likely than over-counting. Five groups in summer and four groups in winter with very deep sighting angles were detected simultaneously on both sides of the plane. The decisions as to which sightings to retain to represent these groups were made randomly. The final datasets contained a record for each

unique sighting, the number of individuals in the group, distance from the trackline and whether the group was detected by the front and/or rear observer.

Detection Function Analysis

Hector's dolphin abundance was estimated using mark-recapture distance sampling (MRDS) techniques (e.g., Buckland et al. 2004, Borchers et al. 2006). As in the ECSI surveys, the range of angles being searched from each observer position was different, therefore similar MRDS methods that were developed for the analysis of that data (MacKenzie & Clement 2016) were used for the analysis of the WCSI survey data. These methods also allow for a lack of independence between the observer detections. The only notable difference between the method applied here with those applied in MacKenzie & Clement (2014) is a slight re-parameterization to allow for more 'symmetric' observer roles which was suggested by Jeff Laake (pers comm). A brief summary of the method is given below.

For the purpose of abundance estimation, the key probability to be determined from the data is the probability of detecting a dolphin group (given that it is present) by at least one of the observer positions on the same side of the aircraft. Denote this as $p_{\bullet}(d_i, s_i)$ where d_i and s_i are the distance and group size measured for the ith group respectively. With the double observer setup, there are four possible outcomes in terms of sighting a dolphin group within a survey transect; 1) sighted by both observers; 2) sighted from the front position, but not the rear; 3) sighted from the rear position, but not the front; or 4) sighted by neither observer. These four outcomes are mutually exclusive and each outcome has an associated probability, the sum of which must equal 1, therefore three of these probabilities can be estimated with the fourth being obtained by subtraction. Note that $p_{\bullet}(d_i, s_i)$ is the sum of the probabilities for the first three outcomes, hence $1 - p_{\bullet}(d_i, s_i)$ is the probability associated with the outcome of a dolphin group not being sighted by either observer.

There are multiple parameterizations that could be used for determining $p_{\bullet}(d_i, s_i)$ (e.g., Laake & Borchers 2004, Buckland et al. 2010, MacKenzie & Clement 2014) and the one used here is:

$$p_{\bullet}(d_i, s_i) = 1 - [1 - p_F(d_i, s_i)][1 - p_{R|NF}(d_i, s_i)] \qquad \text{(Eqn. 1)}$$

where $p_F(d_i, s_i)$ is the probability of the dolphin group being observed from the front observer position and $p_{R|NF}(d_i, s_i)$ is the probability of the dolphin group being observed from the rear position given it *was not* detected by the front observer (*NF*=not front). Note that using this symmetric parameterisation, Eqn. 1 works out to be equivalent to:

$$p_{\bullet}(d_i, s_i) = 1 - [1 - p_R(d_i, s_i)][1 - p_{F|NR}(d_i, s_i)].$$

MacKenzie & Clement (2014) estimated the following components directly $p_F(d_i, s_i)$, $p_{R|NF}(d_i, s_i)$ and $\upsilon_{R|F}(d_i)$, where $\upsilon_{R|F}(d_i)$ is an odds ratio that determines how the odds of detection for the rear observer position changes if a dolphin group was detected from the front observer position. This is 'asymmetric' in the sense that the odds ratio only applies to the detection probability for one observer position. The slight re-parameterization used here

is that the estimated components are $p_{F|NR}(d_i, s_i)$, $p_{R|NF}(d_i, s_i)$ and $\upsilon(d_i)$, where the odds ratio now applies equally for each observer position if a group is detected from the other observer position (hence the symmetry). The interpretation of the odds ratio is similar to before with a value of 1 indicating independent detections.

Note that while the choice of parameterization is likely to have some effect on abundance estimates, MacKenzie & Clement (2016) did not find an appreciable difference in the number of estimated dolphins available in the covered region when the two parameterizations were applied to the ECSI data. For consistency, the symmetric parameterization was used to reanalyse ECSI results for Objective 6.

Covariates

The effects of distance, observer, and group size on detection probabilities were considered by fitting a range of models to the collected data. All covariates were included by using the logit-link function, which is equivalent to performing logistic regression. How detection varied with distance was investigated using three different functional forms (on the logit scale); 1) linear; 2) quadratic; and 3) a natural spline with two internal knots. A natural spline is a method for fitting a flexible, non-parametric curve to data. For each functional relationship for distance ($f(d)$), general equations can be expressed for each of $p_{F|NR}(d_i, s_i)$ and $p_{R|NF}(d_i, s_i)$ (Eqns 2 and 3, respectively) from which six models were considered resulting from the application of various constraints across the regression coefficients.

$$\text{logit}\left(p_{F|NR}(d_i, s_i)\right) = \ln\left(\frac{p_{F|NR}(d_i, s_i)}{1 - p_{F|NR}(d_i, s_i)}\right) = a_1 + \boldsymbol{\beta}_1 f(d_i) + c_1 s_i \qquad (2)$$

$$\text{logit}\left(p_{R|NF}(d_i, s_i)\right) = \ln\left(\frac{p_{R|NF}(d_i, s_i)}{1 - p_{R|NF}(d_i, s_i)}\right) = a_2 + \boldsymbol{\beta}_2 f(d_i) + c_2 s_i \qquad (3)$$

The six models were:

1. different intercept terms and different coefficients for $f(d)$ for each observer position, i.e., $a_1 \neq a_2$, $\boldsymbol{\beta}_1 \neq \boldsymbol{\beta}_2$ and $c_1 = c_2 = 0$.
2. different intercept terms, but the same coefficients for $f(d)$ for each observer position, i.e., $a_1 \neq a_2$, $\boldsymbol{\beta}_1 = \boldsymbol{\beta}_2$ and $c_1 = c_2 = 0$.
3. same intercept and same coefficients for $f(d)$ for each observer position, i.e., $a_1 = a_2$, $\boldsymbol{\beta}_1 = \boldsymbol{\beta}_2$ and $c_1 = c_2 = 0$.
4. as model 1, with constant effect of group size for both observer positions, i.e., $a_1 \neq a_2$, $\boldsymbol{\beta}_1 \neq \boldsymbol{\beta}_2$ and $c_1 = c_2$.
5. as model 2, with constant effect of group size for both observer positions, i.e., $a_1 \neq a_2$, $\boldsymbol{\beta}_1 = \boldsymbol{\beta}_2$ and $c_1 = c_2$.

6. as model 3, with constant effect of group size for both observer positions, i.e., $a_1 = a_2$, $\boldsymbol{\beta}_1 = \boldsymbol{\beta}_2$ and $c_1 = c_2$.

Apparent lack of independence between observers (which may be due to response to cues from the other observer, or unmodelled heterogeneity in detection; Laake & Borchers 2004) was incorporated through the odds ratio $\upsilon(d_i)$ which was modelled on the natural log scale. That is,

$$\ln(\upsilon(d_i)) = a_3 + \beta_3 d_i \qquad (4)$$

noting that only a linear effect with distance was considered. Four models for dependence were considered:

1. full independence, i.e., $a_3 = \beta_3 = 0$ (hence $\upsilon_{R|F}(d_i) = 1$).
2. constant dependence at all distances i.e., $a_3 \neq 0$ and $\beta_3 = 0$.
3. dependence between observer position changes linearly with distance, with full independence at the track line, i.e., $a_3 = 0$ and $\beta_3 \neq 0$ (point independence)
4. as for model 3, but dependence between observers at track line is estimated rather than assuming point independence i.e., $a_3 \neq 0$ and $\beta_3 \neq 0$ (limiting independence, Buckland et al., 2010).

Note that under full independence, and a linear effect of distance, detection models 3, 2, 1 and 4 are equivalent to models 1–4 considered by Manly et al. (1996), though the model likelihoods are formulated slightly differently.

While the model has been described above in terms of detection probabilities that are conditional upon the group not being detected from the other observer position, and an odds ratio, this is equivalent to simply using the detection/nondetection of a dolphin group from one observer position, as the basis for a covariate in the detection function for the other observer position (MacKenzie & Clement 2016). That is, Eqns. 2 or 3 could be combined with Eqn. 4 for a more general expression for the detection probability function. For example, for the front observer position:

$$\text{logit}\left(p_F(d_i, s_i)\right) = a_1 + \boldsymbol{\beta}_1 f(d_i) + c_1 s_i + X_{Ri}(a_3 + \beta_3 d_i)$$

where X_{Ri} indicates whether the *i*th group was detected from the rear observer position (=1 if detected, =0 otherwise).

Model Selection and Diagnostics

For each data set, 72 models were considered for the analysis (3 distance relationships × 6 detection models × 4 dependence models) and compared using Akaike's Information Criterion (AIC; Burnham & Anderson 2002) to determine the level of evidence for each effect. Goodness-of-fit of the detection function was also assessed using quantile-quantile (q-

q) plots along with a Kolmogorov-Smirnov (KS) test and Cramer-von Mises (CvM) test (Buckland et al. 2004).

While AIC was used as the primary model selection tool, other diagnostics were also used to select models based upon the simulation studies conducted by MacKenzie & Clement (2014). Specifically, MacKenzie & Clement (2014) found that in some instances the numerical procedures used to fit the detection function model to the data may produce invalid standard errors for abundance estimates (technically, singular or nearly-singular Hessian matrix), or over-estimate abundance. Over-estimation was particularly problematic for constant dependence and limiting independence models, with a useful diagnostic being the correlation between the intercepts of the detection and dependence components of the model. Extreme correlation values less than -0.95 were associated (but not exclusively so) with over-estimates of abundance. Therefore any models that resulted in abundance estimates that were greater than twice as large as the estimates from similar models (approximately) and with a correlation value between the intercepts of the detection and dependence components of the model approaching -1, were excluded from the set used for final inferences. Models that failed to produce a standard error at all (singular Hessian) or very large standard errors (nearly-singular Hessian) were also excluded.

Model averaging was used to obtain an overall estimate of abundance based upon AIC model weights where there was model selection uncertainty (i.e., models incorporating different factors that have similar levels of support from the data; Anderson 2008). AIC model weights were re-calculated to ensure the weights for the included models summed to 1.0. Stratum-specific detection functions were not considered as few strata would have sufficient sightings to do so.

2.4 Availability Bias

MacKenzie et al. (2012) emphasised the importance of the availability bias for Hector's dolphins given that it is a fundamentally important component for obtaining a reliable estimate of total abundance. Hence, we have undertaken two different methods to assess Hector's dolphin surface availability along the west coast of the South Island.

Helicopter Protocols

Surface availability was estimated using dive/surface intervals of Hector's dolphins collected using a modified sampling protocol and analysis to Slooten et al. (2004) and Clement et al. (2011) and detailed in MacKenzie & Clement (2014). Helicopters searched for dolphins using a similar transect pattern to the fixed-wing airplane; a perpendicular transect was flown out from the shore to approximately 5–10 nmi (depending on location and water depth), the helicopter then travelled parallel to the shore for approximate 1–2 nmi before surveying back towards the shore and maintaining a height of 500 ft. Once a group of dolphins was sighted, the helicopter hovered off to one side or slowly circled the group. While hovering/circling, the observer recorded the duration of the groups' dive and surface intervals into a continuously running dictaphone for approximately ten minutes or until the group disappeared. A range of group sizes, dive behaviours (synchronous, independent, etc.) and age classes were observed.

Our analysis included only complete dive cycles (i.e. dropping the first surface and last dive interval as needed) to calculate the average time a group was visible near the surface and average time below the surface.

From Laake & Borchers (2004), the probability of a group being available (P_α) can be calculated from dive cycle data by:

$$P_\alpha = 1 - \frac{\bar{b}\exp\left(-t/\bar{b}\right)}{\bar{u}+\bar{b}} \qquad (5)$$

where $\bar{b}$ is the average time below the surface, $\bar{u}$ the average time up or near the surface and t is the time frame for which the group is within the view of the observers from the aircraft. The standard error for P_α can be calculated as:

$$SE(P_\alpha) = \sqrt{\left[\frac{\bar{b}\exp\left(t/\bar{b}\right)}{\left(\bar{u}+\bar{b}\right)^2}\right]^2 V_{\bar{u}} - 2\bar{u}\bar{b}\left[1+\frac{t\left(\bar{u}+\bar{b}\right)}{\bar{u}\bar{b}}\right]V_{\bar{u}\bar{b}} + \bar{u}^2\left[1+\frac{t\left(\bar{u}+\bar{b}\right)}{\bar{u}\bar{b}}\right]^2 V_{\bar{b}}} \qquad (6)$$

where $V_{\bar{u}}$ and $V_{\bar{b}}$ are the variances for $\bar{u}$ and $\bar{b}$ respectively, and $V_{\bar{u}\bar{b}}$ is the covariance for the two means.

Regional estimates of availability were calculated and incorporated into estimates of total abundance. Only Hector, Greymouth and Okarito Lagoon strata were sampled, as the low number of survey sightings within the other three regional areas did not justify the longer search times needed to collect sufficient dive profile sample sizes. The value from the Hector strata was applied to the nearby Whanganui Inlet strata and the Greymouth estimate applied to Jackson Bay and Milford Sound.

Circle-back protocols

The second field method was a variation of the 'circle-back' method originally proposed by Hiby (1999) using a single fixed-wing aircraft (see details in MacKenzie & Clement 2014). Circle-backs were carried out from the survey plane while on-effort and flying along transects. Once a dolphin group was sighted by an observer, and the other observer on the same side had an opportunity to detect the same group (e.g. 5–10 secs), the observer would call 'availability'. After marking the location on his GPS, the pilot continued to fly along the transect for another 20 secs (about 1 nmi) and call 'off-effort' before beginning a gentle turn that would bring the plane onto the next parallel transect. Note that the pilot did not conduct a 2-minute standard rate turn for the circle-backs. The pilot would back-track along the parallel transect for approximately 2–3 nmi (1–2 mins), using the GPS mark to ensure sufficient space of the plane to turn back onto the original transect, flatten its wings and re-survey the transect well before the location of the original sighting and the off-effort mark. The same procedure was repeated for a second circle-back with observers going back 'on-effort' when the plane crossed over the original GPS mark and carrying on surveying the rest of the transect. It took between 5.25 to 9.83 minutes (e.g. mean= 3.8 min per circle in summer and 4.4 min per circle in winter) to complete two full circle-backs from the time of the original sighting until the plane was back on-effort.

Circle-back sightings and duplicates were verified in a similar manner to on-effort sightings. To aid in the identification of any re-sightings of the original group, observers kept detailed records of all circle-back activities. The observer who called availability would record the

original sighting details using the normal survey protocol. All observers would note the time in their dictaphones when off-effort was called by the pilot while continuing to survey until the plane started to turn. Observers would rest as the plane back-tracked. As the plane turned back onto the original transect, observers would note the time and circle number and then begin surveying according to normal on-effort protocols. The resulting sightings (corrected for perpendicular distance off the transect line) and all circle-back information (off-effort location, circle starts, etc.) were visually plotted in ArcGIS to help with identification (Figure 3).

The mean distance that a Hector's dolphin group might move within the time it took the plane to complete a circle was estimated by measuring the width of a random assortment of helicopter observation tracks (see *Helicopter Protocols* above) from the start of a dive sighting observation to the end. Over summer, groups observed by helicopter moved a mean distance of 580 m over an average duration of 10.6 minutes (i.e. 54.9 m per min) and 543 m over 10.2 min in winter (i.e. 53.0 m per min). These movement estimates meant that any re-sightings of a group could conservatively occur within a 500 m circle radius of the original sighting, given the average length of time needed to complete two full circle-backs (Figure 3). In combination with all the collected information (e.g. group size, duplicate sightings, comments on cues, etc.), most re-sightings greater than this radius were considered a new group.

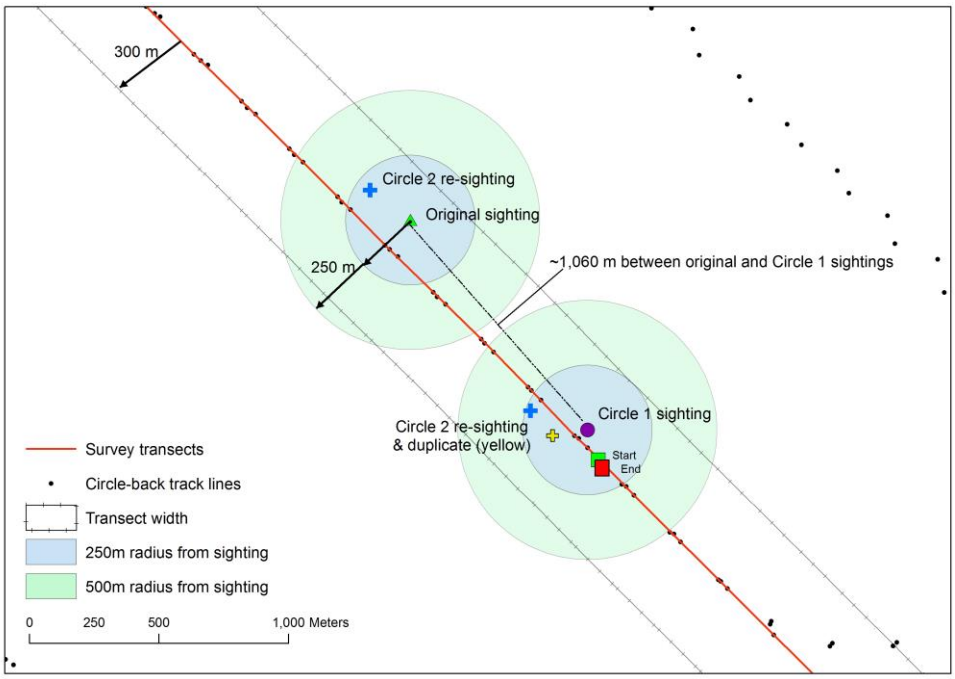

Figure 3: Examples of circle-back redetections in which the mean distance that the original group (and any subsequent sightings) might have moved over the course of a circle-back were based on estimates from helicopter observations. Two circular zones (e.g. 250 m and 500 m) were drawn around each potential sighting to help with determining redetections on subsequent circle-back attempts. Note that these examples show dolphin movement along the transect line and from one side of the plane to the other.

Other groups recorded after or before the original sighting by other observers could also be used as part of the availability calculation. Analysis of this method could be difficult in high

density areas where multiple groups were sighted in the same general location. As a result, observers had the ability to cancel an availability call if they observed multiple groups before or after the original call.

With this method, the idea is to re-survey the same portion of transect with the exact same protocol (i.e. flying at 500 ft travelling 100 knts) in an attempt to re-detect the same group of dolphins with each new pass. Information about availability comes from the proportion of passes where the original dolphin group was observed on (or near) the surface. It is assumed that the dolphin group remains within the transect strip being surveyed during each of the circle-backs (note that dolphin movements may be along, or to the other side of, the transect and not necessarily directly out of the transect area). This assumption would be difficult to relax without information on finer-scale dolphin movement patterns. Dolphin groups may not be detected either because they have become unavailable (i.e., dived below the surface), or they have been available but missed by the observers. This aspect can be easily accounted for by using the information from the detection function collected from the on-effort sightings. For example, if P_α is the availability probability and $E(p_\bullet(s_i))$ is the expected probability of detecting a group of size s_i from at least one of the observer positions, then the probability of redetecting the group during a circle-back is $P_\alpha E(p_\bullet(s_i))$ and the probability of not detecting the group would be $1-P_\alpha E(p_\bullet(s_i))$. Note that the inclusion of $E(p_\bullet(s_i))$ to account for perception bias in the estimation of availability does not amount to double-correcting for perception bias when it is also included for abundance estimation.

Estimates and standard errors for P_α can be obtained using maximum likelihood techniques. An important point is that for a group to be included in the circle-back data, it must be detected at least once; however inclusion of the initial group sighting in the analysis would result in availability being over-estimated. Therefore, estimates of P_α were obtained by using the number of circle-backs and number of redetections of a group after its first detection. This estimation procedure differs from that originally used by Hiby (1999).

The effect of region (corresponding to the same regions used in the helicopter-based surveys) and offshore stratum (0–4 nmi vs further out) on availability were investigated. Availability was modelled as:

$$\text{logit}(P_\alpha) = \delta_0 + \boldsymbol{\delta}_1 \mathit{Region} + \delta_2 \mathit{Offshore} \qquad (7)$$

The *Region* factor has more than two levels and requires multiple indicator variables to represent these effects; hence the regression coefficient is indicated as a vector quantity (i.e., in bold font). Water colour was not considered due to the manner in which the availability estimates would be included into the abundance estimates (by region and offshore strata). Four models were fit to the data by including different combinations of the covariates, and ranked according to AIC. For the purpose of abundance estimation, the stratum-specific availability estimates (both regionally and offshore) were modelled averaged and these model averaged estimates of availability were used in the estimation of abundance.

Note that the availability estimates may vary depending on which detection function is used to estimate $E(p_\bullet(s_i))$; hence the procedure outlined above was repeated for each detection function that was used to estimate abundance. That is, for each detection function that was ranked highly according to AIC, it was used to estimate both the number of dolphins in the

area covered by the survey and the probability of them being available. These were then combined to estimate total abundance.

Note that similar truncation rules used for the detection function sighting data were applied to the circle-back data, whereby if the initial sighting was outside the truncation distances for the front or rear observer, the circle-back data for that group was not used. Therefore, for the analyses where only the sighting data between 0.071-0.300 km is used for both observers, availability is estimated from a subset of the full circle-back data set.

2.5 Abundance Estimation

Based upon Laake & Borchers (2004) and Buckland et al. (2010), dolphin abundance was estimated in the following manner.

The number of dolphins within the area of stratum *k* covered by the surveys is estimated using a Horvitz-Thomson type estimator, i.e.,

$$\hat{N}_{ck} = \sum_{i=1}^{n_k} \frac{s_i}{E\left(p\ (s_i)\right)} \qquad (8)$$

where n_k is the number of groups detected in the stratum, s_i is the size of the *i*th group and $E(p_{\bullet}(s_i))$ is the expected probability of the *i*th group being detected given its size, which is obtained from the detection function analysis.

The number of *available* dolphins (i.e., near the surface with a non-zero change of detection by the observers in the plane) within the stratum is therefore

$$\hat{N}_{ak} = \frac{A_k \hat{N}_{ck}}{a_k} \qquad (9)$$

where, A_k is the total area of the stratum; $a_k = 2wL_k$ is the area covered by the survey transects with *w* being the truncated width (0.3 km) and L_k the total transect length flown. Accounting for availability, that total number of dolphins within a stratum is therefore:

$$\hat{N}_k = \frac{\hat{N}_{ak}}{\hat{P}_{ak}} \qquad (10)$$

with total abundance being:

$$\hat{N} = \sum_{k=1}^{K} \hat{N}_k \qquad (11)$$

Details on the calculation of the standard errors are given in Mackenzie & Clement (2014), but note that they are extensions of the methods used by Buckland et al. (2010). It should also be noted that given that some strata share parameters (either through the detection function or availability estimates), the standard errors from the stratum-specific abundance estimates cannot be simply combined to obtain the standard error for total dolphin abundance.

As there may be model selection uncertainty associated with the detection function analysis, which would lead to different estimates of abundance (and availability using the circle-back

data), AIC-based model averaging was used to combine the abundance estimates resulting from each detection function model (Burnham & Anderson, 2002; Anderson 2008, see SM Section B). Four sets of abundance estimates are obtained: those resulting from the full and reduced distance data sets with either circle-back or dive-profile-based estimates of availability. Model averaging calculations were used to combine the four estimates into a single result, where each set of estimates were given equal weight. Note that by using these calculations, variation in the different abundance estimates is incorporated into the standard error of the final estimate. Based upon an averaged estimate of abundance ($\hat{N}$) and its associated standard error (*SE*), the lower and upper limits of a Wald-lognormal 95% confidence interval were calculated.

2.6 Distribution Analyses

Density surface modelling (DSM; Buckland et al. 2004) was used to examine Hector's dolphin distribution and potentially identify seasonal shifts, where distribution is defined as those areas with a non-negligible predicted density. DSM techniques combine the survey data with a spatial analysis to model how density at the time of surveying varies across a region according to spatial and habitat variables (e.g. bathymetry, distance from shore) while taking into account the probability of detecting the animals (Gomez de Segura et al. 2007). Further corrections can be made to account for dolphin availability. It is important to note that a DSM produces a predicted density surface based upon line-transect data from a single survey. Spatial and habitat information is used to explain variability in where dolphins were sighted at the time of the survey, which results in the prediction surface. The estimated prediction surface may be sensitive to the exact location of the sightings with an alternative data set leading to a different prediction surface. Even though a DSM may use habitat variables, it is not a study of habitat preferences of the animals. The results cannot be used to make broad conclusions about the habitat preference of Hector's dolphins.

DSM protocols

Separate DSMs were developed to estimate the summer- and winter-time distribution of Hector's dolphins. For each season, the DSM was developed by using the top-ranked detection function model from the full distance sampling data set. Easting, northing and distance from shore were included as covariates for the DSM. Inclusion of depth was also attempted although led to unrealistic results. The analyses were undertaken within the statistical software R using a combination of custom code and the package *dsm* (v.2.2.9). Transect lines were divided into segments approximately 1 km long and 0.6 km wide, with the easting and northing coordinates for the centre point of the segment determined. Values for easting, northing and distance from shore were obtained from a prediction grid with 5×5 km cells. Dolphin abundance was estimated for each transect segment based upon the number of dolphins sighted in each segment, the estimated detection function and helicopter-based estimates of regional availability (Buckland et al. 2004). That is:

$$\hat{N}_i = \sum_{j=1}^{n_i} \frac{s_{ij}}{E\left(p_{\bullet}\left(s_{ij}\right)\right)\hat{P}_{ak}}$$

where $\hat{N}_i$ is the estimated abundance for segment *i*, n_i is the number of groups in the segment, s_{ij} is the size of the *j*th group in the segment, $E(p_\bullet(s_{ij}))$ is the expected probability of detecting a group of size s_{ij}, and $\hat{P}_{ak}$ is the estimated availability probability for stratum *k* (which segment *i* is contained within).

A generalised additive model (GAM) was used to model the segment-specific abundance estimates based on the above covariates (with easting and northing entered as a bivariate spline term). The results of the GAM were used to predict dolphin density across the study region using the prediction grid that was defined at a scale of 5×5 km cells. No attempts were made to simplify the GAM by removing covariates that appeared to have little effect on the prediction surface.

Standard errors were obtained using a parametric bootstrap to accommodate uncertainty in both the detection function and DSM. It was implemented in the following steps:

1. Fit the detection function and DSM to the observed data to estimate the number of individual dolphins.
2. Refit DSM to estimate the density of available dolphin groups (as sightings are made of groups not individually).
3. Generate locations of available (e.g., near surface) groups using a random Poisson point process where the process intensity is obtained from the adjusted group-level DSM fitted in step 2.
4. Determine perpendicular distance of the group from nearest transect line. Retain groups that are within the area covered by the survey (i.e., within 0.3 km). Other groups are not retained as they have no chance of being sighted.
5. Randomly generate group size using a group-size frequency table. This table is based on the observed group frequency, with correction for detection probability being different for different group sizes. That is, $\hat{f}_s = \frac{n_s / E[p_\bullet(s)]}{\hat{N}_{gc}}$, where $\hat{f}_s$ is the estimated frequency of group size *s*, n_s is the number of observed groups of size *s*, $E(p_\bullet(s))$ is the expected probability of detecting a group of size *s* within the covered area and $\hat{N}_{gc}$ is the estimated number of groups within the covered area
6. Using the detection function estimated in step 1, determine the probability of detection for each group given its distance from the line and size, from each observer position.
7. Generate a Bernoulli random variable (i.e., 0 or 1) to indicate whether each group was sighted from each observer position.
8. Using the groups sighted at least once, refit the detection function model used in step 1 to obtain detection estimates pertinent to the generated (i.e., bootstrapped) data set.
9. For each region, generate a new availability estimate by drawing a random value from a logit-normal distribution with mean and standard deviation equal to the logit-transformed regional availability estimate and associated standard error.
10. Using the detection function model fit in step 8, and availability estimates obtained in step 9, refit the DSM used in step 1 to obtain a predicted density surface (of individuals) for the bootstrap data set.
11. Repeat steps 3–10 a sufficiently large number of times. The standard deviation of summaries calculated from the bootstrapped DSMs can be used to approximate the standard errors of the corresponding quantities from the DSM for the real data.

MacKenzie et al. (2012) noted from simulation studies that resulting maps from a DSM analysis were sensitive to the exact location of detections when using a 5 × 5 km prediction grid and recommended that for the purpose of robust inferences about distribution, coarser spatial scales (e.g., cells of hundreds of square kilometres) should be used. While the results of the DSM are presented at the prediction grid scale, extreme caution is advised in terms of using the DSM to make such fine scale inferences because the maps will be sensitive to where dolphins were observed at the time of the survey. Changes in where dolphins were sighted, either due to dolphin movement or random chance, may lead to quite different maps. Hence, the DSM results may not accurately represent distribution information over a longer timeframe. It is recommended that the results from the prediction grid that have been aggregated to the courser scale of the strata be used for distribution and abundance inferences. A grid cell was defined to be associated with a defined stratum if its centroid was within the stratum boundaries, therefore given the resolution of the prediction grid, stratum areas are slightly different compared to those used previously.

Maps of the DSM results are expressed as relative densities. That is, the estimated density for a grid cell or stratum relative to the overall density;

$$\frac{\hat{N}_k / A_k}{\hat{N} / A},$$

as a means to identify areas of relative higher or lower density that are robust to the magnitude of absolute abundance estimates. Values over 1 indicate areas with densities that are greater than the overall average. Note that the relative density can also be interpreted as the fraction of the total population in cell or stratum *k*, relative to the proportion of the total area contained within that cell or stratum, i.e.,

$$\frac{\hat{N}_k / \hat{N}}{A_k / A}.$$

2.7 South Island Abundance and Distribution Estimate

Estimated Hector's dolphin abundance for the entire South Island was estimated from the results of the most recent SCSI, ECSI and WCSI aerial surveys. Upon review, it was decided to reanalyse the SCSI and ECSI survey data for methodological consistency with WCSI. Slightly different protocols were used in the SCSI survey, requiring a slightly different approach to the detection function analysis, particularly due to the very low number of on-effort sightings. In addition, availability was only assessed using dive-cycle information collected from helicopter surveys. Details of the methods employed for the SCSI reanalysis are given in Section A of the SM. As identical field protocols were used for the WCSI and ECSI surveys, the ECSI data was reanalysed using the same methods used for the WCSI.

Summer and winter abundance estimates were averaged to give a single estimate for each region. The seasonal estimates for ECSI and WCSI are independent; therefore, the standard error for the regional average can be calculated in the regular manner. The seasonal estimates for the SCSI are not independent because of the shared detection function; therefore the

standard error for the averaged SCSI estimate was calculated by considering the seasonal surveys as separate strata and using the same calculations detailed in Section 2.5.

A South Island-wide abundance estimate was calculated by summing together the independent regional estimates. Note that this estimate excludes harbours and sounds that were not surveyed (most notably Akaroa Harbour and the Marlborough Sounds).

The South Island-wide distribution of Hector's dolphin was obtained from the DSMs fit to the ECSI and WCSI sighting data. Summer and winter DSMs were combined to provide an indication of their general distribution. The seasonal DSMs were combined by averaging the relative density for each 5 km cell in the prediction grid, and associated standard errors calculated from the seasonal results. For consistency with the abundance estimates, the DSMs for the seasonal ECSI results were re-estimated using the symmetric parameterisation of the detection function (see SM Figures T.9-T.10). A single DSM was also calculated for the SCSI using sightings from both the August and March survey periods due to the low number of sightings (see SM Figure S.4). Sightings obtained during the auxiliary surveys conducted to increase the sample size for detection function estimation were also included in the DSM. The ability to incorporate the additional sightings from outside the main survey is one advantage of using a DSM. Only a bivariate spline term was used to create the SCSI DSM as the total number of sightings was small (i.e., depth and distance from shore were not included).

3. RESULTS

3.1 WCSI Abundance Estimates

A summary of the summer and winter sighting data is given in Table 4 and Section C of the SM report. These sample sizes far exceed the recommended minimum of 60–80 sightings for estimating abundance (Buckland et al. 2001). For the front observer position during the summer survey, 13 sightings were left truncated (i.e., had distances less than 0.071 km) and nine sightings were right truncated (distance more than 0.300 km). For the rear observer position, four sightings had a recorded angle greater than 90 degrees that were set equal to 90 degrees (0 km) and two sightings were right truncated, both of which had also been sighted by the front observer. Note that some groups for which the front observer sightings were left-truncated may have also been detected by the rear observer so the group is retained in the data set as a single sighting. An additional 72 sightings made from the rear observer position were left truncated for the data analysis where both observers had the same viewing area (i.e. reduced data set).

From the winter survey, 23 sightings were left truncated (i.e., had distances less than 0.071 km) for the front observer position and four sightings were right truncated (distance more than 0.300 km). One sighting was right truncated for the rear observer position. Ninety-two sightings made from the rear observer position were left truncated for the data analysis where both observers had the same viewing area.

Histograms are provided in the SM (Section D) of the verified distance data prior to any truncation and histograms of the distance data after truncation for both surveys. Note that for the reduced data set where all data was left truncated, distances have been rescaled such that the original distance of 0.071 km now equals 0 km.

Table 4: Summary of the sighting data from the summer and winter aerial surveys. 'Verified' indicates the numbers post-verification; 'Full' indicates the numbers used in the full analysis where sightings were left truncated at 0.071 km for the front observer position and right truncated at 0.300 km for both observer positions; and 'Reduced' indicates the numbers used in the subset analysis where sightings were left truncated at 0.071 km and right truncated at 0.300 km for both observer positions. Note that the number of groups sighted from both positions are also included in the front and rear totals.

	Summer			Winter		
	Verified	**Full**	**Reduced**	**Verified**	**Full**	**Reduced**
Total Sightings	265	250	178	281	272	184
Total Front	170	158	158	182	155	155
Total Rear	215	207	135	237	232	144
Both (duplicates)	131	115	115	138	115	115
Individuals	547	513	373	544	519	355
Average Group Size	2.06	2.05	2.10	1.94	1.91	1.93
SD Group Size	1.41	1.39	1.40	1.48	1.47	1.28
Range Group Size	1–9	1–9	1–8	1–16	1–16	1–11
Transect Length (km)	**4001**	**4001**	**4001**	**4307**	**4307**	**4307**

Detection function analysis

Summer

The top 10 models (as ranked by AIC) for the full summer data set are given in Table 5. Most of the AIC weight is associated with the top three models, but lower ranked models also have non-negligible weight; therefore the top seven models were used to produce model averaged estimates of abundance after adjusting their AIC model weights such that they sum to 1. The correlations between the intercepts of the detection and dependence functions are well away from -1, giving no indication of potential over-estimation. All of the top seven models have different detection functions with distance for each observer position, and group size as a covariate for detection. While the top-ranked model assumes linear relationships with distance, the second-ranked model assumes quadratic relationships. Overall, the linear quadratic relationships have most of the support. The top two models assume point independence of the detections, while the third-fifth ranked models assume limiting independence.

Plots of the fitted detection functions and empirical histograms of detection rates do not indicate any systematic concerns about lack of fit for any of the top seven models, particularly for $p_{\bullet}(d_i, s_i)$, which is the most relevant in terms of estimating abundance. The fitted detection functions for the top ranked model is presented in Figure 4 for illustration and the plots for all seven models are given in Section E of the SM. The q-q plots (Figure 5 and SM Section E) and goodness of fit tests (Table 6) do not indicate any evidence of lack of fit for the top six models.

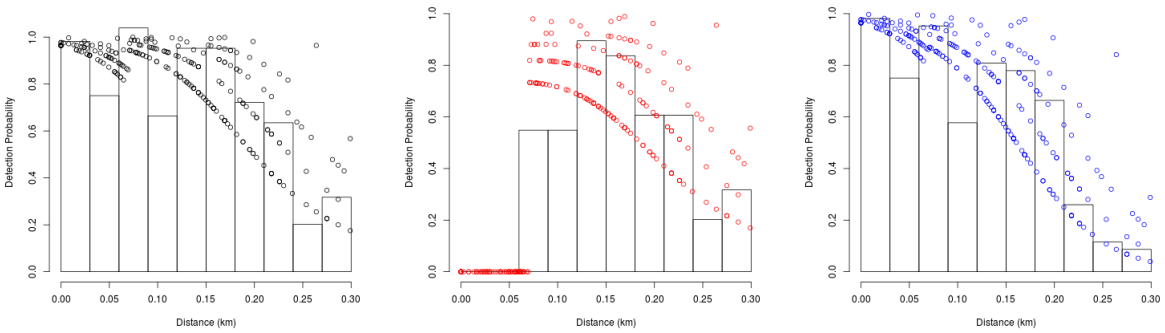

Figure 4: Fitted detection functions and histograms of empirical detection probabilities from the top ranked model in Table 5. Left is $p_{\bullet}(d_i, s_i)$, centre is $p_F(d_i, s_i)$, and right is $p_R(d_i, s_i)$.

Table 5: Top 10 AIC-ranked models for the detection function analysis for sightings between 0-0.3 km from the transect line in the summer. Model components identify the structure of the detection function model; $f(d)$ is the functional relationship with distance on the logit scale (L=linear, Q=quadratic, S=Spline), Obs indicates whether the intercept term is different for each observer position (Y=Yes, N=No), $\beta_1 \neq \beta_2$ indicates whether the regression coefficients for the effect of distance on detection is different for each observer position (Y= Yes, N= No), Size indicates whether group size has an effect on detection (Y=Yes, N=No) and Dep. indicates the form of dependence in detection between observer positions (FI=Full Independence, C = Constant Dependence, P = Point Independence and L= Limiting Independence). ΔAIC is the relative difference in AIC values, wgt is the AIC model weight, wgt* is the adjusted AIC weight for the models used for inference, -2*l* is twice the negative log-likelihood, pars. is the number of parameters in the model, $\hat{N}_{cg}$ is the estimated number of dolphin groups in the covered area, $SE(\hat{N}_{cg})$ is the standard error for $\hat{N}_{cg}$, corr. is the correlation between the intercepts of the detection and dependence components of the model and ESW is the effective strip width accounting for detection and perception bias.

Model Components													
$f(d)$	Obs	$\beta_1 \neq \beta_2$	Size	Dep.	ΔAIC	wgt	wgt*	-2*l*	pars.	$\hat{N}_{cg}$	$SE(\hat{N}_{cg})$	corr.	ESW
L	Y	Y	Y	P	0.00	0.31	0.32	241.80	6	346	25		0.216
Q	Y	Y	Y	P	0.69	0.22	0.23	238.49	8	370	40		0.203
L	Y	Y	Y	L	0.85	0.20	0.21	240.65	7	318	16	-0.75	0.235
Q	Y	Y	Y	L	2.44	0.09	0.09	238.24	9	354	65	-0.90	0.212
S	Y	Y	Y	L	3.46	0.06	0.06	235.26	11	337	54	-0.51	0.223
S	Y	Y	Y	P	3.56	0.05	0.05	237.36	10	338	31		0.222
L	Y	Y	Y	C	4.59	0.03	0.03	246.39	6	420	81	-0.83	0.178
Q	Y	Y	Y	C	5.84	0.02		243.64	8	405	74	-0.61	
S	Y	Y	Y	C	7.05	0.01		240.85	10	393	79	0.05	
L	Y	Y	N	P	11.50	0.00		255.30	5	347	24		

Table 6: Goodness of fit tests for top seven ranked models for the detection function analysis of the full summer data set. Given are the Cramer-von Mises (CvM) and Kolmogorov-Smirnov (KS) tests with associated p-values.

Model Rank	CvM	p-value	KS	p-value
1	0.085	0.67	0.050	0.56
2	0.062	0.80	0.048	0.61
3	0.055	0.84	0.048	0.61
4	0.057	0.84	0.048	0.61
5	0.054	0.85	0.048	0.61
6	0.055	0.84	0.048	0.61
7	0.101	0.58	0.048	0.61

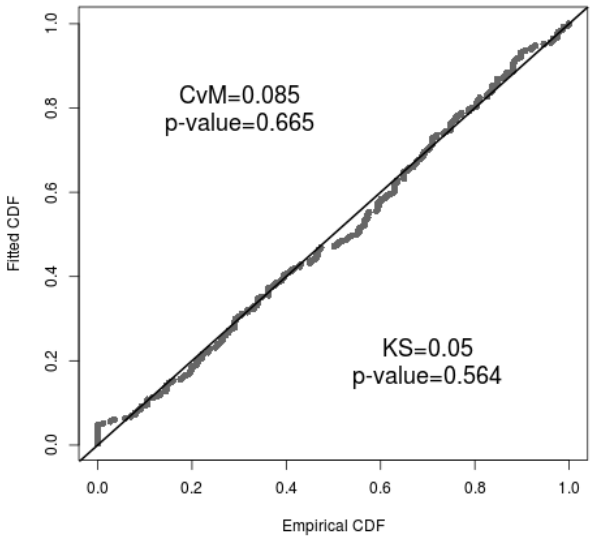

Figure 5: Q-Q plot of the fitted and empirical cumulative density functions (CDF) for the top ranked model of the detection function analysis of the full summer data.

Using the detection data from the portion of the transect that can be viewed from both observer positions (0.071-0.300 km) results in similar conclusions to using the fuller data set (Table 7). The correlation between the intercepts of the detection and dependence components of the model for the third-eighth ranked models are -0.97, -0.93, -1.00, -0.89, -0.98 and -0.91, respectively. These are all in the region where unrealistically high abundance estimates might be obtained (MacKenzie et al. 2012). The point estimates of $\hat{N}_{cg}$ from the third, fifth and seventh ranked models are very comparable to those from the top two models, while the estimates from sixth and eighth ranked models are only moderately higher. However, the estimate from the fourth ranked is approximately 60% higher than those from the top two models. The associated standard errors for the estimates from the fourth and sixth ranked models are also much higher (particularly for the fourth model). Given these results, it was decided to exclude the fourth ranked model from the final inferences; and model averaging has been performed based upon the models ranked 1–3 and 5–8.

Plots of the fitted detection functions and empirical histograms of detection rates for the seven models used for model averaging do not indicate any systematic concerns about lack of fit for either model, particularly for $p_{\bullet}(d_i, s_i)$, which is most relevant for abundance estimation. Figure 6 presents the fitted detection functions for the top-ranked model with Section F (SM) including the plots for all seven models. The q-q plots (Figure 7 and SM Section F) and goodness of fit tests do not indicate any evidence of lack of fit for the seven models either (Table 8).

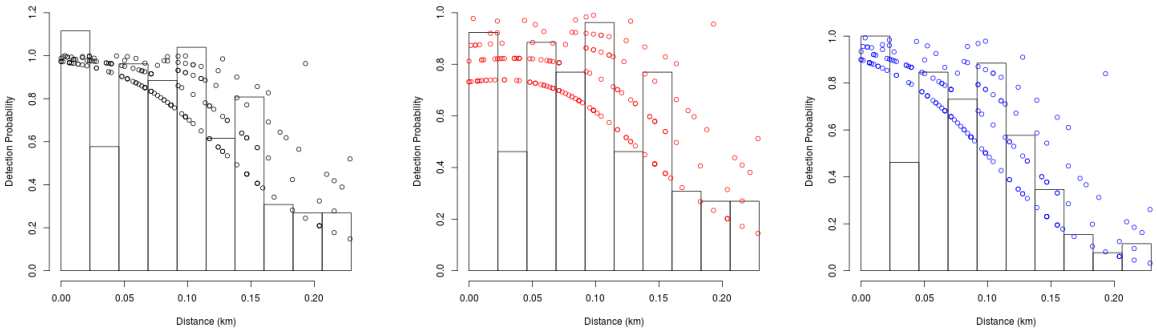

Figure 6: Fitted detection functions and histograms of empirical detection probabilities from the top ranked model in Table 7. Left is $p_{\bullet}(d_i, s_i)$, centre is $p_F(d_i, s_i)$, and right is $p_R(d_i, s_i)$. Note that distance from the transect line has been rescaled such that an original distance of 0.071 km is now 0 km.

Table 7: Top 10 AIC-ranked models for the detection function analysis for sightings reduced to between 0.071-0.300 km from the transect line in the summer. Model components identify the structure of the detection function model; $f(d)$ is the functional relationship with distance on the logit scale (L=linear, Q=quadratic, S=Spline), Obs indicates whether the intercept term is different for each observer position (Y=Yes, N=No), $\beta_1 \neq \beta_2$ indicates whether the regression coefficients for the effect of distance on detection is different for each observer position (Y= Yes, N= No), Size indicates whether group size has an effect on detection (Y=Yes, N=No) and Dep. indicates the form of dependence in detection between observer positions (FI=Full Independence, C = Constant Dependence, P = Point Independence and L= Limiting Independence). ΔAIC is the relative difference in AIC values, wgt is the AIC model weight, wgt* is the adjusted AIC weight for the models used for inference, -2*l* is twice the negative log-likelihood, pars. is the number of parameters in the model, $\hat{N}_{cg}$ is the estimated number of dolphin groups in the covered area, $SE(\hat{N}_{cg})$ is the standard error for $\hat{N}_{cg}$, corr. is the correlation between the intercepts of the detection and dependence components of the model and ESW is the effective strip width accounting for detection and perception bias.

Model Components													
$f(d)$	Obs	$\beta_1 \neq \beta_2$	Size	Dep.	ΔAIC	wgt	wgt*	-2*l*	pars.	$\hat{N}_{cg}$	$SE(\hat{N}_{cg})$	corr.	ESW
L	Y	Y	Y	P	0.00	0.37	0.44	245.14	6	260	20		0.157
Q	Y	Y	Y	P	1.50	0.18	0.21	242.63	8	258	22		0.158
L	Y	Y	Y	L	1.69	0.16	0.19	244.83	7	247	25	-0.97	0.165
Q	Y	Y	Y	C	2.05	0.13		243.19	8	504	361	-0.93	
Q	Y	Y	Y	L	3.50	0.06	0.08	242.63	9	258	88	-1.00	0.158
S	Y	Y	Y	C	5.20	0.03	0.03	242.34	10	349	157	-0.89	0.117
S	Y	Y	Y	L	5.39	0.03	0.03	240.52	11	253	45	-0.98	0.161
L	Y	Y	Y	C	5.56	0.02	0.03	250.69	6	345	109	-0.91	0.118
S	Y	Y	Y	P	9.20	0.00		246.34	10	236	18		
L	Y	Y	N	P	10.35	0.00		257.48	5	261	20		

Table 8: Goodness of fit tests for top seven ranked models for the detection function analysis of the reduced summer data set. Given are the Cramer-von Mises (CvM) and Kolmogorov-Smirnov (KS) tests with associated p-values.

Model Rank	CvM	p-value	KS	p-value
1	0.093	0.62	0.058	0.60
2	0.081	0.69	0.050	0.77
3	0.081	0.69	0.047	0.82
5	0.081	0.69	0.050	0.77
6	0.086	0.66	0.045	0.87
7	0.085	0.66	0.044	0.89
8	0.194	0.28	0.071	0.32

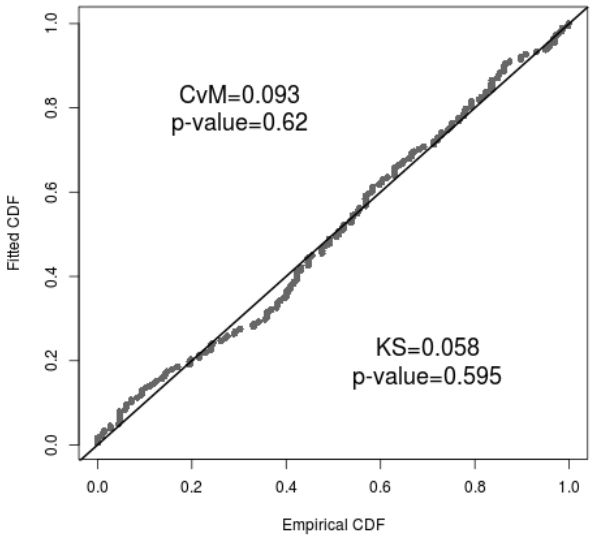

Figure 7: Q-Q plot of the fitted and empirical cumulative density functions (CDF) for the top ranked model of the detection function analysis of the reduced summer data. Q-Q plots for all seven models used for model averaging are given in SM Section F.

Winter

The top 10 models (as ranked by AIC) for the full winter data set are given in Table 9. The AIC weight values suggest that no single model has much greater support than other models, with the values gradually declining from 0.29. Therefore, the top eight models were used to produce model averaged estimates of abundance after adjusting their AIC model weights such that they sum to 1. The most extreme correlation between the intercepts of the detection and dependence functions is -0.92 for the fifth-ranked model, which does not have an unusually high abundance estimate. The correlation was more than -0.85 for all other highly ranked models. All of the top eight models have different detection functions with distance for each observer position and group size as a covariate for detection. Three of the top-four models assume a quadratic relationship between distance and detection, with the second, fifth and ninth ranked models assuming a linear relationship. The remainder of the top-eight models involved the spline function for distance. Constant dependence, point independence and limiting independence models all featured in the top-ranked models, although none of the top-ranked models included the assumption of full independence of sightings from each observer position.

Plots of the fitted detection functions and empirical histograms of detection rates do not indicate any systematic concerns about lack of fit for any of the top eight models, particularly for $p_{\bullet}(d_i, s_i)$, which is the most relevant in terms of estimating abundance (SM Section G). The fitted detection functions for the top ranked model is presented in Figure 8 for illustration and the plots for all eight models are given in Section G of the Supplemental Material. The q-q plots (Figure 9 and SM Section G) and goodness of fit tests (Table 10) do not indicate any evidence of lack of fit for the top eight models.

Using the winter detection data from the portion of the transect that can be viewed from both observer positions (0.071-0.300 km) results in similar conclusions to using the fuller data set (Table 11). The correlation between the intercepts of the detection and dependence components of the model for the first, third, fourth, fifth, seventh, eighth and tenth ranked models are -0.93,-0.98, -0.95, -0.91, -0.98, -0.89 and -1.00, respectively. The estimated number of groups in the covered region is unrealistically high for the tenth-ranked model, while estimates from the other models with extreme correlation values are not unreasonable (although the estimate from the top-ranked model is substantially higher than other estimates). However for these models, with the exception of the fourth-ranked model, the associated standard errors are very large (i.e., CVs more than 30% compared to CVs less than 15% for the other models). Therefore, the first, third, fifth, seventh, eighth and tenth ranked models were excluded due to the combination of extreme correlations and high standard errors.

Plots of the fitted detection functions and empirical histograms of detection rates for the four models used for model averaging do not indicate any systematic concerns about lack of fit, particularly for $p_{\bullet}(d_i, s_i)$, which is most relevant for abundance estimation. Figure 10 presents the fitted detection functions for the top-ranked model with SM Section H including the plots for all four models. The q-q plots (Figure 11 and SM Section H) and goodness of fit tests do not indicate any evidence of lack of fit for the four models (Table 12).

Table 9: Top 10 AIC-ranked models for the detection function analysis for winter sightings between 0-0.3 km from the transect line. Model components identify the structure of the detection function model; $f(d)$ is the functional relationship with distance on the logit scale (L=linear, Q=quadratic, S=Spline), Obs indicates whether the intercept term is different for each observer position (Y=Yes, N=No), $\beta_1 \neq \beta_2$ indicates whether the regression coefficients for the effect of distance on detection is different for each observer position (Y= Yes, N= No), Size indicates whether group size has an effect on detection (Y=Yes, N=No) and Dep. indicates the form of dependence in detection between observer positions (FI=Full Independence, C = Constant Dependence, P = Point Independence and L= Limiting Independence). ΔAIC is the relative difference in AIC values, wgt is the AIC model weight, wgt* is the adjusted AIC weight for the models used for inference, -2*l* is twice the negative log-likelihood, pars. is the number of parameters in the model, $\hat{N}_{cg}$ is the estimated number of dolphin groups in the covered area, $SE(\hat{N}_{cg})$ is the standard error for $\hat{N}_{cg}$, corr. is the correlation between the intercepts of the detection and dependence components of the model and ESW is the effective strip width accounting for detection and perception bias.

Model Components													
$f(d)$	Obs	$\beta_1 \neq \beta_2$	Size	Dep.	ΔAIC	wgt	wgt*	-2*l*	pars.	$\hat{N}_{cg}$	$SE(\hat{N}_{cg})$	corr.	ESW
Q	Y	Y	Y	P	0.00	0.29	0.29	238.07	8	402	29		0.203
L	Y	Y	Y	P	0.62	0.21	0.21	242.69	6	427	32		0.191
Q	Y	Y	Y	C	1.15	0.16	0.16	239.21	8	475	99	-0.43	0.172
Q	Y	Y	Y	L	1.97	0.11	0.11	238.04	9	474	134	-0.85	0.172
L	Y	Y	Y	L	2.28	0.09	0.09	242.35	7	416	48	-0.92	0.196
S	Y	Y	Y	P	2.82	0.07	0.07	236.89	10	399	32		0.205
S	Y	Y	Y	C	4.01	0.04	0.04	238.08	10	477	148	-0.07	0.171
S	Y	Y	Y	L	4.61	0.03	0.03	236.68	11	400	20	-0.18	0.204
L	Y	Y	Y	C	8.14	0.00		250.20	6	541	110	-0.83	
Q	Y	Y	N	P	11.98	0.00		252.04	7	396	28		

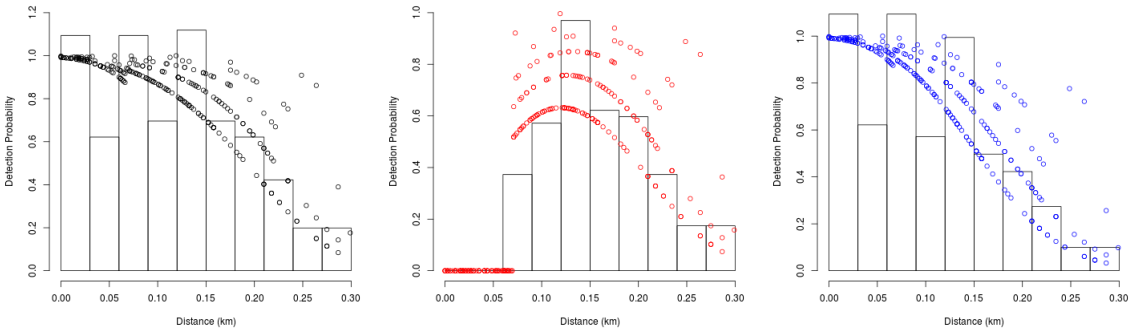

Figure 8: Fitted detection functions and histograms of empirical detection probabilities from the top ranked model in Table 9. Left is $p_{\bullet}(d_i, s_i)$, centre is $p_F(d_i, s_i)$, and right is $p_R(d_i, s_i)$.

Table 10: Goodness of fit tests for top eight ranked models for the detection function analysis of the full winter data set. Given are the Cramer-von Mises (CvM) and Kolmogorov-Smirnov (KS) tests with associated p-values.

Model Rank	CvM	p-value	KS	p-value
1	0.050	0.87	0.037	0.84
2	0.069	0.76	0.039	0.79
3	0.087	0.65	0.043	0.69
4	0.056	0.84	0.036	0.86
5	0.077	0.706	0.041	0.74
6	0.037	0.95	0.035	0.90
7	0.054	0.85	0.036	0.88
8	0.048	0.89	0.038	0.83

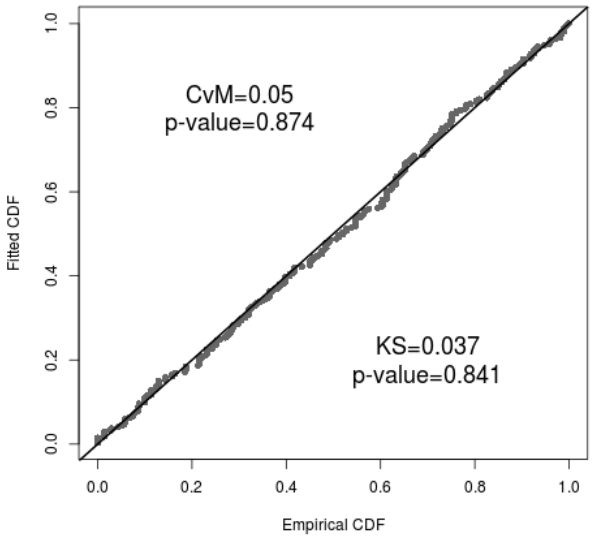

Figure 9: Q-Q plot of the fitted and empirical cumulative density functions (CDF) for the top ranked model of the detection function analysis of the full winter data.

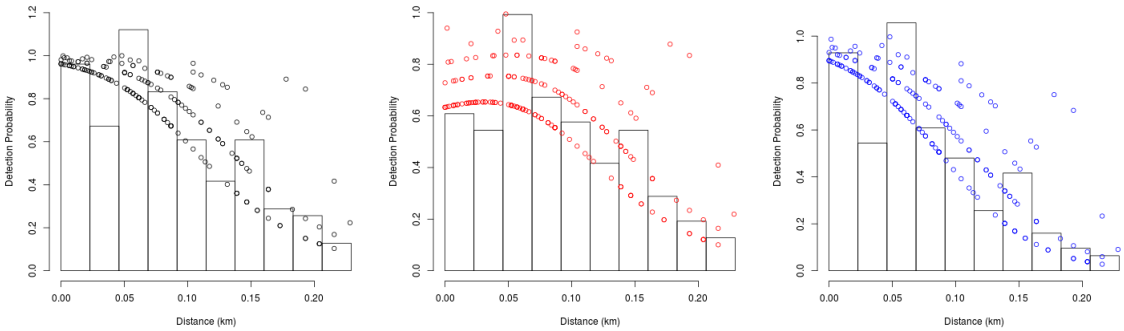

Figure 10: Fitted detection functions and histograms of empirical detection probabilities from the top model used for model averaging in Table 11. Left is $p_{\bullet}(d_i, s_i)$, centre is $p_F(d_i, s_i)$, and right is $p_R(d_i, s_i)$. Note that distance from the transect line has been rescaled such that an original distance of 0.071 km is now 0 km.

Table 11: Top 10 AIC-ranked models for the detection function analysis for sightings reduced to between 0.071-0.300 km from the transect line in the winter. Model components identify the structure of the detection function model; $f(d)$ is the functional relationship with distance on the logit scale (L=linear, Q=quadratic, S=Spline), Obs indicates whether the intercept term is different for each observer position (Y=Yes, N=No), $\beta_1 \neq \beta_2$ indicates whether the regression coefficients for the effect of distance on detection is different for each observer position (Y= Yes, N= No), Size indicates whether group size has an effect on detection (Y=Yes, N=No) and Dep. indicates the form of dependence in detection between observer positions (FI=Full Independence, C = Constant Dependence, P = Point Independence and L= Limiting Independence). ΔAIC is the relative difference in AIC values, wgt is the AIC model weight, wgt* is the adjusted AIC weight for the models used for inference, -2*l* is twice the negative log-likelihood, pars. is the number parameters in the model, $\hat{N}_{cg}$ is the estimated number of dolphin groups in the covered area, $SE(\hat{N}_{cg})$ is the standard error for $\hat{N}_{cg}$, corr. is the correlation between the intercepts of the detection and dependence components of the model and ESW is the effective strip width accounting for detection and perception bias.

Model Components													
$f(d)$	Obs	$\beta_1 \neq \beta_2$	Size	Dep.	ΔAIC	wgt	wgt*	-2*l*	pars.	$\hat{N}_{cg}$	$SE(\hat{N}_{cg})$	corr.	ESW
Q	Y	Y	Y	C	0.00	0.33		249.69	8	545	317	-0.93	
L	Y	Y	Y	P	0.22	0.29	0.67	253.91	6	312	26		0.135
Q	Y	Y	Y	L	1.68	0.14		249.38	9	379	176	-0.98	
L	Y	Y	Y	L	2.18	0.11	0.25	253.88	7	318	47	-0.95	0.132
S	Y	Y	Y	C	3.84	0.05		249.54	10	413	164	-0.91	
Q	Y	Y	Y	P	4.66	0.03	0.07	254.36	8	300	29		0.140
S	Y	Y	Y	L	4.81	0.03		248.50	11	434	299	-0.98	
L	Y	Y	Y	C	7.89	0.01		261.58	6	454	134	-0.89	
S	Y	Y	Y	P	8.06	0.01	0.01	253.75	10	296	26		0.142
Q	Y	Y	N	C	9.66	0.00		261.35	7	31193	862801	-1.00	

Table 12: Goodness of fit tests for the four detection function models used for model averaging from the reduced winter data set. Given are the Cramer-von Mises (CvM) and Kolmogorov-Smirnov (KS) tests with associated p-values.

Model Rank	CvM	p-value	KS	p-value
2	0.058	0.83	0.047	0.82
4	0.065	0.78	0.051	0.73
6	0.069	0.76	0.058	0.57
9	0.049	0.88	0.054	0.66

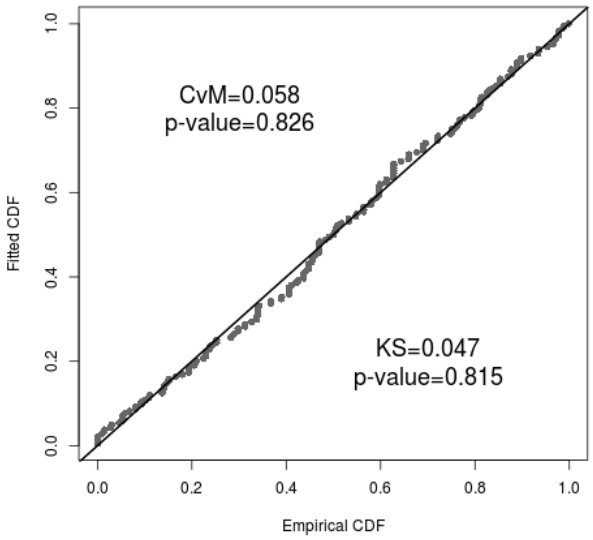

Figure 11: Q-Q plot of the fitted and empirical cumulative density functions (CDF) for the top detection function model used for model averaging of the reduced winter data. Q-Q plots for all four models used for model averaging are given in SM Section H.

Availability Bias

Helicopter Dive Profiles

During the summer survey, dive information was collected on 62 different dolphin groups equating to over 1000 complete dive cycles (Table 13, Figure 12). On a regional level, dive sightings ranged from 19 to 22 groups and 340 to 356 dive cycles. Availability estimates would suggest that there is some regional variation, with availability possibly being lower in the Okarito Lagoon region (Figure 13). In the ECSI survey (MacKenzie & Clement 2014), it was determined that fixed objects are within an observers view for about six seconds on average, hence *t*=6 has been used to correct for availability bias when estimating abundance (Table 13).

During the winter survey, dive information was collected on 72 different dolphin groups equating to 675 complete dive cycles. On a regional level, dive sightings ranged from 19 to 31 groups and 124 to 318 dive cycles (Table 14, Figure 14). Availability estimates for winter are very similar to those for summer, with availability in Okarito Lagoon strata estimated lower than for Hector and Grey strata. As for the summer surveys, t=6 has been used to correct for availability bias when estimating abundance.

Table 13: Summary of summer dive-cycle data and availability estimates. Estimates presented are the number of groups data were collected on (*n*), average time on or near the surface ($\bar{u}$), average dive time ($\bar{b}$), variance for the average surface time ($V_{\bar{u}}$), variance for the average dive time ($V_{\bar{b}}$) and covariance between average surface and dive time ($V_{\bar{u}\bar{b}}$). All times are given in seconds. Estimated probability of a group being available ($\hat{P}_{\alpha}$) for *t* = 6 seconds and associated standard error (*SE*).

Area	*n*	$\bar{u}$	$\bar{b}$	$V_{\bar{u}}$	$V_{\bar{b}}$	$V_{\bar{u}\bar{b}}$	$\hat{P}_{\alpha}$	*SE*
Hector	21	26.1	34.8	15.8	22.4	14.9	0.52	0.03
Greymouth	22	21.3	32.6	18.1	24.1	10.1	0.50	0.06
Okarito Lagoon	19	19.6	43.5	10.1	83.8	13.1	0.40	0.07

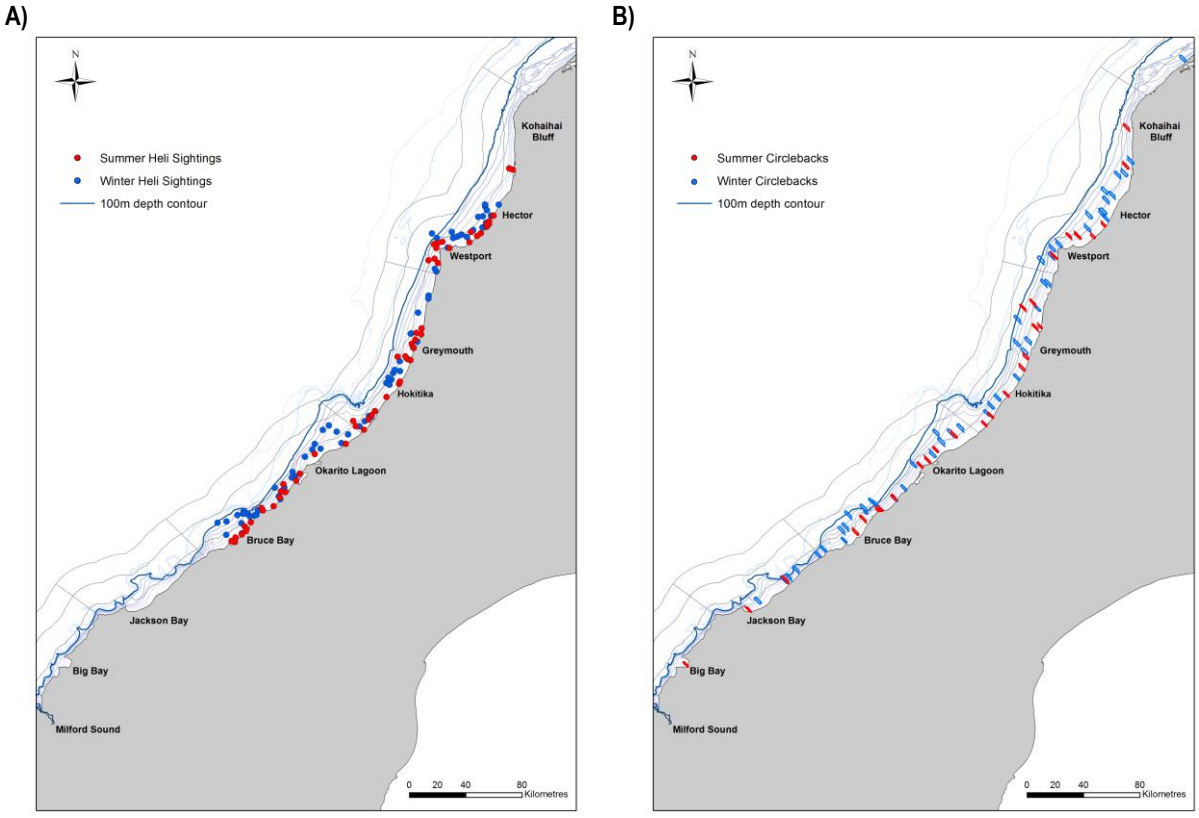

Figure 12: A comparison between the locations of summer (red dots) and winter (blue dotes) availability sightings from A) helicopter observations and B) circle-back track attempts within each of the survey stratum.

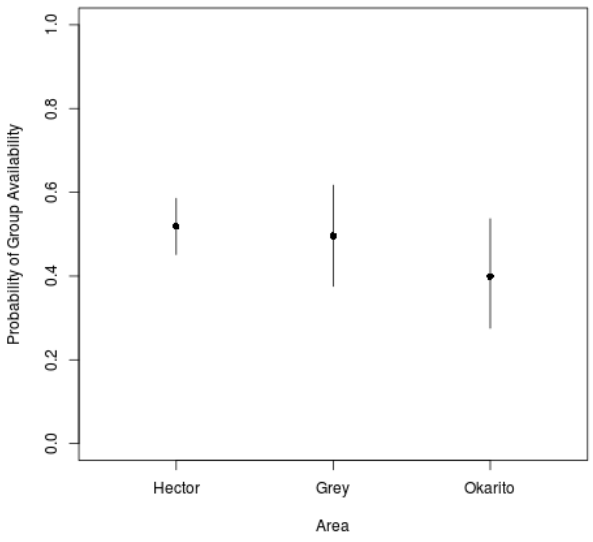

Figure 13: Estimated availability and 95% confidence intervals obtained from the dive-cycle data during summer.

Table 14: Summary of winter dive-cycle data and availability estimates. Estimates presented are the number of groups data were collected on (*n*), average time on or near the surface ($\bar{u}$), average dive time ($\bar{b}$), variance for the average surface time ($V_{\bar{u}}$), variance for the average dive time ($V_{\bar{b}}$) and covariance between average surface and dive time ($V_{\bar{u}\bar{b}}$). All times are given in seconds. Estimated probability of a group being available ($\hat{P}_{\alpha}$) for *t* = 6 seconds and associated standard error (*SE*).

Area	*n*	$\bar{u}$	$\bar{b}$	$V_{\bar{u}}$	$V_{\bar{b}}$	$V_{\bar{u}\bar{b}}$	$\hat{P}_{\alpha}$	*SE*
Hector	22	25.2	34.3	13.0	19.0	8.9	0.52	0.04
Greymouth	19	59.4	63.7	154.4	171.1	3.9	0.53	0.09
Okarito Lagoon	31	45.4	89.9	16.7	88.7	13.4	0.38	0.03

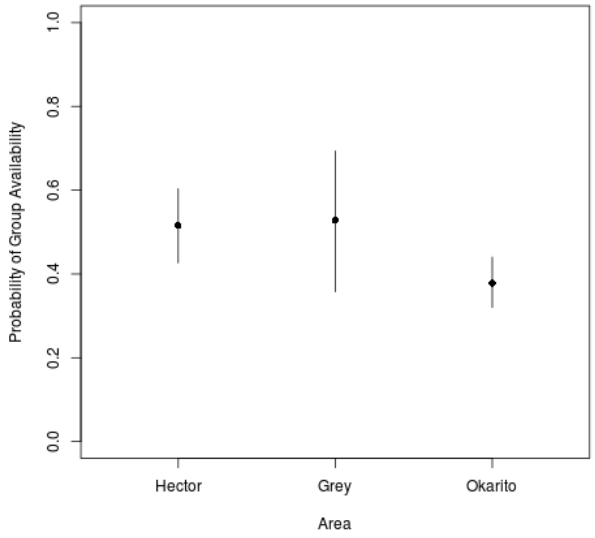

Figure 14: Estimated availability and 95% confidence intervals obtained from the dive-cycle data during winter.

Circle-back Redetections

Following data verification, 27 circle-backs were completed during the summer survey (see Figure 12) with data used from 56 dolphin groups (often multiple groups were spotted during a circle-back), and a total of 99 attempts to resight dolphin groups with 48 successful redetections by at least one observer (after first sighting of the group). The seven detection function models identified in Table 5 were used in the modelling of the circle-back data. Investigation of the two factors of interest (region and offshore) resulted in similar AICs regardless of the detection function used (Table 15). Only the results from the top-model in Table 5 are presented here, although model selection summaries for all detection functions are given in Section I of the Supplemental Material.

For each detection function used, model averaged estimates of availability were calculated (Table 16), which were then used to estimate dolphin abundance. Standard errors have not been presented in Table 16, but are included with the stratum-specific abundance estimates from each detection function (SM Section J).

Table 15: Model selection summary for factors affecting summer availability as assessed from circle-back protocol, using the detection function from the top-ranked model in Table 5. Parameters given are the relative difference in AIC values (ΔAIC), AIC model weights (*w*), twice the negative log-likelihood (*-2l*) and the number of parameters in the model (*NPar*). The '.' model assumes equal availability across all factors.

Model	ΔAIC	*w*	*-2l*	*NPar*
.	0.00	0.48	108.40	1
offshore	0.89	0.31	107.30	2
region	2.60	0.13	107.00	3
region+offshore	3.69	0.08	106.09	4

Table 16: Model averaged availability estimates from the full summer data for each detection function. Column labels indicate the order of the detection function models in Table 5 with the values in parentheses indicating the corresponding adjusted AIC model weight for each detection function model.

Coastal Section	Offshore Stratum (nmi)	1 (0.32)	2 (0.23)	3 (0.21)	4 (0.09)	5 (0.06)	6 (0.05)	7 (0.03)
Whanganui Inlet	0–4	0.66	0.70	0.62	0.67	0.66	0.65	0.75
	4–12	0.57	0.60	0.53	0.58	0.56	0.56	0.64
	12–20	0.57	0.60	0.53	0.58	0.56	0.56	0.64
Hector	0–4	0.66	0.70	0.62	0.67	0.66	0.65	0.75
	4–12	0.57	0.60	0.53	0.58	0.56	0.56	0.64
	12–20	0.57	0.60	0.53	0.58	0.56	0.56	0.64
Greymouth	0–4	0.67	0.71	0.62	0.69	0.66	0.66	0.79
	4–12	0.58	0.61	0.54	0.59	0.57	0.57	0.68
	12–20	0.58	0.61	0.54	0.59	0.57	0.57	0.68
Okarito Lagoon	0–4	0.70	0.75	0.65	0.72	0.69	0.69	0.84
	4–12	0.61	0.65	0.56	0.62	0.60	0.60	0.74
	12–20	0.61	0.65	0.56	0.62	0.60	0.60	0.74
Jackson Bay	0–4	0.67	0.71	0.62	0.69	0.66	0.66	0.79
	4–12	0.58	0.61	0.54	0.59	0.57	0.57	0.68
	12–20	0.58	0.61	0.54	0.59	0.57	0.57	0.68
Milford Sound	0–4	0.67	0.71	0.62	0.69	0.66	0.66	0.79
	4–12	0.58	0.61	0.54	0.59	0.57	0.57	0.68
	12–20	0.58	0.61	0.54	0.59	0.57	0.57	0.68

For the reduced summer analysis, 31 dolphin groups with 53 attempted resightings and 21 successful redetections were used. The seven detection function models identified in Table 7 were used in the modelling of the circle-back data. As for the full data set model selection, results were very similar for all detection functions; hence only the results from the top-model in Table 7 are presented here (Table 17), with summaries for all detection functions given in Section K (Supplemental Material).

For each detection function used, model averaged estimates of availability were calculated (Table 18), which were then used to estimate dolphin abundance. Standard errors have not been presented in Table 18, but are included with the stratum-specific abundance estimates from each detection function (SM- Section L).

Table 17: Model selection summary for factors affecting summer availability as assessed from circle-back protocol, using the detection function from the top-ranked model in Table 7. Results presented are the relative difference in AIC values (ΔAIC), AIC model weights (*w*), twice the negative log-likelihood (-2*l*) and the number of parameters in the model (*NPar*). The '.' model assumes equal availability across all factors.

Model	ΔAIC	*w*	-2*l*	*NPar*
.	0.00	0.63	59.95	1
offshore	1.91	0.24	59.86	2
region	3.75	0.10	59.70	3
region+offshore	5.64	0.04	59.59	4

Table 18: Model averaged availability estimates from the reduced summer data for each detection function. Column labels indicate the order of the detection function models in Table 7 with the values in parentheses indicating the corresponding adjusted AIC model weight for each detection function model.

Coastal Section	Offshore Stratum (nmi)	1 (0.44)	2 (0.21)	3 (0.19)	5 (0.08)	6 (0.03)	7 (0.03)	8 (0.03)
Whanganui Inlet	0–4	0.60	0.59	0.57	0.59	0.70	0.52	0.75
	4–12	0.57	0.57	0.54	0.57	0.68	0.50	0.73
	12–20	0.57	0.57	0.54	0.57	0.68	0.50	0.73
Hector	0–4	0.60	0.59	0.57	0.59	0.70	0.52	0.75
	4–12	0.57	0.57	0.54	0.57	0.68	0.50	0.73
	12–20	0.57	0.57	0.54	0.57	0.68	0.50	0.73
Greymouth	0–4	0.59	0.58	0.55	0.58	0.70	0.51	0.75
	4–12	0.56	0.55	0.53	0.55	0.68	0.49	0.73
	12–20	0.56	0.55	0.53	0.55	0.68	0.49	0.73
Okarito Lagoon	0–4	0.60	0.60	0.57	0.60	0.72	0.52	0.77
	4–12	0.57	0.57	0.54	0.57	0.70	0.50	0.75
	12–20	0.57	0.57	0.54	0.57	0.70	0.50	0.75
Jackson Bay	0–4	0.59	0.58	0.55	0.58	0.70	0.51	0.75
	4–12	0.56	0.55	0.53	0.55	0.68	0.49	0.73
	12–20	0.56	0.55	0.53	0.55	0.68	0.49	0.73
Milford Sound	0–4	0.59	0.58	0.55	0.58	0.70	0.51	0.75
	4–12	0.56	0.55	0.53	0.55	0.68	0.49	0.73
	12–20	0.56	0.55	0.53	0.55	0.68	0.49	0.73

Following data verification of the winter data, 46 circle-backs were completed during the winter survey (see Figure 12), with data used from 82 dolphin groups (often multiple groups were spotted during a circle-back) and a total of 143 attempts to resight dolphin groups with 48 successful redetections by at least one observer. The eight detection function models identified in Table 9 were used in the modelling of the circle-back data. Investigation of the two factors of interest (region and offshore) resulted in similar AICs regardless of the detection function used (Table 19). Only the results from the top-model in Table 9 are presented here, although model selection summaries for all detection functions are given in SM Section M.

For each detection function used, model averaged estimates of availability were calculated (Table 20), which were then used to estimate dolphin abundance. Standard errors have not been presented in Table 20, but are included with the stratum-specific abundance estimates from each detection function (SM Section N).

Table 19: Model selection summary for factors affecting winter availability as assessed from circle-back protocol, using the detection function from the top-ranked model in Table 9. Parameters given are the relative difference in AIC values (ΔAIC), AIC model weights (*w*), twice the negative log-likelihood (-2*l*) and the number of parameters in the model (*NPar*). The '.' model assumes equal availability across all factors.

Model	ΔAIC	*w*	-2*l*	*NPar*
.	0.00	0.59	145.35	1
offshore	1.83	0.24	145.18	2
region	3.22	0.12	144.57	3
region+offshore	4.83	0.05	144.18	4

Table 20: Model averaged availability estimates from the full winter data for each detection function. Column labels indicate the order of the detection function models in Table 9 with the values in parentheses indicating the corresponding adjusted AIC model weight for each detection function model.

Coastal Section	Offshore Stratum (nmi)	1 (0.29)	2 (0.21)	3 (0.16)	4 (0.11)	5 (0.09)	6 (0.07)	7 (0.04)	8 (0.03)
Whanganui Inlet	0–4	0.49	0.58	0.52	0.58	0.51	0.48	0.49	0.58
	4–12	0.51	0.60	0.54	0.60	0.53	0.50	0.50	0.60
	12–20	0.51	0.60	0.54	0.60	0.53	0.50	0.50	0.60
Hector	0–4	0.49	0.58	0.52	0.58	0.51	0.48	0.49	0.58
	4–12	0.51	0.60	0.54	0.60	0.53	0.50	0.50	0.60
	12–20	0.51	0.60	0.54	0.60	0.53	0.50	0.50	0.60
Greymouth	0–4	0.51	0.60	0.54	0.60	0.53	0.51	0.51	0.60
	4–12	0.53	0.62	0.56	0.62	0.55	0.52	0.53	0.62
	12–20	0.53	0.62	0.56	0.62	0.55	0.52	0.53	0.62
Okarito Lagoon	0–4	0.50	0.59	0.54	0.59	0.52	0.50	0.50	0.59
	4–12	0.52	0.61	0.55	0.61	0.54	0.52	0.52	0.61
	12–20	0.52	0.61	0.55	0.61	0.54	0.52	0.52	0.61
Jackson Bay	0–4	0.51	0.60	0.54	0.60	0.53	0.51	0.51	0.60
	4–12	0.53	0.62	0.56	0.62	0.55	0.52	0.53	0.62
	12–20	0.53	0.62	0.56	0.62	0.55	0.52	0.53	0.62
Milford Sound	0–4	0.51	0.60	0.54	0.60	0.53	0.51	0.51	0.60
	4–12	0.53	0.62	0.56	0.62	0.55	0.52	0.53	0.62
	12–20	0.53	0.62	0.56	0.62	0.55	0.52	0.53	0.62

For the reduced winter analysis, 47 dolphin groups with 82 attempted resightings and 27 successful redetections were used. The four detection function models identified in Table 11 were used in the modelling of the circle-back data. As for the full data set model selection, results were very similar for all detection functions; hence only the results from the top-model in Table 11 are presented here (Table 21), with summaries for all detection functions given in SM Section O.

For each detection function used, model averaged estimates of availability were calculated (Table 22), which were then used to estimate dolphin abundance. Standard errors have not been presented in Table 22, but are included with the stratum-specific abundance estimates from each detection function (SM- Section P).

Table 21: Model selection summary for factors affecting winter availability as assessed from circle-back protocol, using the detection function from the top model in Table 11 used for model averaging. Results presented are the relative difference in AIC values (ΔAIC), AIC model weights (*w*), twice the negative log-likelihood (-2*l*) and the number of parameters in the model (*NPar*). The '.' model assumes equal availability across all factors.

Model	ΔAIC	*w*	-2*l*	*NPar*
.	0.00	0.55	82.28	1
offshore	1.91	0.21	82.19	2
region	2.34	0.17	80.62	3
region+offshore	4.23	0.07	80.51	4

Table 22: Model averaged availability estimates from the reduced winter data for each detection function. Column labels indicate the order of the detection function models in Table 11 with the values in parentheses indicating the corresponding adjusted AIC model weight for each detection function model.

Coastal Section	Offshore Stratum (nmi)	2 (0.67)	4 (0.25)	6 (0.07)	10 (0.01)
Whanganui Inlet	0–4	0.51	0.53	0.49	0.42
	4–12	0.53	0.54	0.51	0.44
	12–20	0.53	0.54	0.51	0.44
Hector	0–4	0.51	0.53	0.49	0.42
	4–12	0.53	0.54	0.51	0.44
	12–20	0.53	0.54	0.51	0.44
Greymouth	0–4	0.58	0.59	0.55	0.48
	4–12	0.59	0.60	0.57	0.49
	12–20	0.59	0.60	0.57	0.49
Okarito Lagoon	0–4	0.58	0.59	0.56	0.48
	4–12	0.60	0.61	0.57	0.50
	12–20	0.60	0.61	0.57	0.50
Jackson Bay	0–4	0.58	0.59	0.55	0.48
	4–12	0.59	0.60	0.57	0.49
	12–20	0.59	0.60	0.57	0.49
Milford Sound	0–4	0.58	0.59	0.55	0.48
	4–12	0.59	0.60	0.57	0.49
	12–20	0.59	0.60	0.57	0.49

WCSI Abundance estimates

Summer

Summer estimates of dolphin abundance, after correcting for each availability bias, are given in Table 23. Details of the stratum-specific estimates from each detection function are given in the SM (Sections J and L when using circle-back based estimates of availability, and Section Q when using dive-cycle based availability estimates). Table 24 contains the abundance estimates obtained by averaging the four sets of estimates, which provides an estimate of Hector's dolphin summer abundance along the WCSI (out to 20 nmi) of 5490 (CV: 26%; 95% CI: 3319–9079).

Winter

Winter estimates of dolphin abundance, after correcting for each availability bias, are given in Table 25. Details of the stratum specific estimates from each detection function are given in the SM (Sections N and P when using circle-back based estimates of availability, and Section R when using dive-cycle based availability estimates). Table 26 contains the abundance estimates obtained by averaging the four sets of estimates, which provides an estimate of Hector's dolphin winter abundance along the WCSI (out to 20 nmi) of 5802 (CV: 21%; 95% CI: 3879–8679).

Table 23: Model averaged summer abundance estimates and standard errors for each stratum from data of sightings between 0-0.3 km (Full Data) and 0.071-0.3 km (Reduced Data). Given are the estimated abundance of Hector's dolphins (corrected for availability bias; $\hat{N}_k$ using the availability estimates from the dive-cycle data and circle-back data).

		Full Data				Reduced Data			
		Dive Cycle		Circle-back		Dive Cycle		Circle-back	
Coastal Section	**Offshore Stratum (nmi)**	$\hat{N}_k$	**SE**	$\hat{N}_k$	**SE**	$\hat{N}_k$	**SE**	$\hat{N}_k$	**SE**
Whanganui Inlet	0–4								
	4–12								
	12–20								
Hector	0–4	1 431	311	1 118	275	1 509	372	1 313	394
	4–12	549	403	499	399	398	261	363	265
	12–20								
Greymouth	0–4	1 433	350	1 053	249	1 330	410	1 130	385
	4–12	59	55	50	49	83	80	74	74
	12–20								
Okarito Lagoon	0–4	1 856	467	1 051	236	1 845	536	1 228	354
	4–12	804	605	522	416	837	670	583	494
	12–20								
Jackson Bay	0–4	231	140	169	102	147	133	125	114
	4–12								
	12–20								
Milford Sound	0–4	39	30	28	22	55	44	46	37
	4–12								
	12–20								
Total		**6 402**	**1 169**	**4 491**	**883**	**6 203**	**1 356**	**4 862**	**1 223**

Table 24: Estimated summer abundance of Hector's dolphins in each stratum and overall obtained from averaging the two different data sets and two methods of estimating availability. Results presented are the average estimate and associated standard error, along with the lower and upper limits of a 95% confidence interval.

Coastal Section	Offshore Stratum (nmi)	$\overline{\hat{N}}_k$	SE	Lower	Upper
Whanganui Inlet	0–4				
	4–12				
	12–20				
Hector	0–4	1 343	372	788	2 287
	4–12	452	347	119	1 717
	12–20				
Greymouth	0–4	1 237	385	681	2 245
	4–12	66	67	13	343
	12–20				
Okarito Lagoon	0–4	1 495	550	744	3 004
	4–12	687	572	166	2 847
	12–20				
Jackson Bay	0–4	168	129	44	640
	4–12				
	12–20				
Milford Sound	0–4	42	35	10	177
	4–12				
	12–20				
Total		**5 490**	**1 433**	**3 319**	**9 079**

Table 25: Model averaged winter abundance estimates and standard errors for each stratum from data of sightings between 0-0.3 km (Full Data) and 0.071-0.3 km (Reduced Data). Given are the estimated abundance of Hector's dolphins (corrected for availability bias; $\hat{N}_k$ using the availability estimates from the dive-cycle data and circle-back data).

		Full Data				Reduced Data			
Coastal Section	**Offshore Stratum (nmi)**	**Dive Cycle**		**Circle-back**		**Dive Cycle**		**Circle-back**	
		$\hat{N}_k$	**SE**	$\hat{N}_k$	**SE**	$\hat{N}_k$	**SE**	$\hat{N}_k$	**SE**
Whanganui Inlet	0–4	189	148	185	145	270	204	271	217
	4–12								
	12–20								
Hector	0–4	786	210	771	219	606	168	606	234
	4–12	271	94	257	95	173	79	167	90
	12–20								
Greymouth	0–4	1 708	437	1 648	386	1 573	386	1440	378
	4–12	500	292	468	272	703	402	625	371
	12–20								
Okarito Lagoon	0–4	1 653	400	1 162	303	1 835	406	1 199	342
	4–12	550	211	374	150	540	213	343	152
	12–20								
Jackson Bay	0–4	607	273	586	256	596	306	545	285
	4–12								
	12–20								
Milford Sound	0–4								
	4–12								
	12–20								
Total		6 265	1 198	5 452	1 073	6 296	1 028	5 197	1 101

Table 26: Estimated winter abundance of Hector's dolphins in each stratum and overall obtained from averaging the four sets of results from the two different data sets and methods of estimating availability. Results presented are the average estimate and associated standard error, along with the lower and upper limits of a 95% confidence interval.

Coastal Section	Offshore (nmi)	Stratum	$\overline{\hat{N}}_k$	SE	Lower	Upper
Whanganui Inlet	0–4		229	186	57	925
	4–12					
	12–20					
Hector	0–4		692	226	371	1 292
	4–12		217	101	91	519
	12–20					
Greymouth	0–4		1 593	410	969	2 616
	4–12		574	352	190	1 736
	12–20					
Okarito Lagoon	0–4		1 463	466	795	2 690
	4–12		452	207	192	1 062
	12–20					
Jackson Bay	0–4		583	282	238	1 430
	4–12					
	12–20					
Milford Sound	0–4					
	4–12					
	12–20					
Total			5 802	1 205	3 879	8 679

3.2 WCSI Distribution Results

Hector's dolphins along the west coast were generally found quite close to shore (i.e. within 2 nmi) and in relatively shallow depths both seasons (Table 27, Figure 15a, Figure 16). Approximately 70% and 57% of all summer and winter sightings (respectively) were within waters less than 30 m. Yet on both surveys, several dolphins were observed in waters greater than 100 m. Most of these deeper sightings were within the Okarito Lagoon and Jackson Bay strata where the continental shelf meanders much closer to the coast than most northern regions (Figure 15a).

The WCSI population noticeably shifts further offshore from summer to winter, although it is not as substantial a shift as observed for the ECSI population (MacKenzie & Clement 2014). Several sightings of dolphins were observed at distances further than previous offshore distribution results (about 5.3 nmi) by Rayment et al. (2010b; Figure 17). Our furthest survey sightings were approximately 12 km (6.5 nmi) in summer and 17.7 km (9.5 nmi) in winter (Table 27), and several groups were observed as far offshore as 20.5 km (10.9 nmi) during winter training flights off Hector between 16 and17 June 2015. MPI observers have also reported Hector's dolphins as far offshore as 16.5 km (8.8 nmi) along this coastline (Figure 17). As no sightings occurred within the 12–20 nmi stratum, the survey is likely to have encompassed the full offshore limits of this west coast population.

Table 27: The mean and maximum distance from shore (km) and depths (m) at which summer and winter survey sightings of Hector's dolphin occurred.

	Summer		Winter		Summer		Winter	
	Distance offshore (km)		Distance offshore (km)		Depth (m)		Depth (m)	
Stratum	**Mean**	**Max**	**Mean**	**Max**	**Mean**	**Max**	**Mean**	**Max**
WCSI	3.3	12.0	5.1	17.7	29.4	160.0	42.3	200.0
Whanganui Inlet	-	-	2.8	3.2	-	-	40.0	40.0
Hector	3.1	9.1	5.3	16.9	26.0	70.0	29.1	90.0
Greymouth	2.3	12.0	4.9	17.7	15.3	70.0	27.8	90.0
Okarito Lagoon	4.1	10.9	5.4	16.2	39.5	160.0	55.2	170.0
Jackson Bay	1.8	3.7	4.4	7.4	21.1	30.0	115.0	200.0
Milford Sound	0.4	0.4	-	-	10.0	10.0	-	-

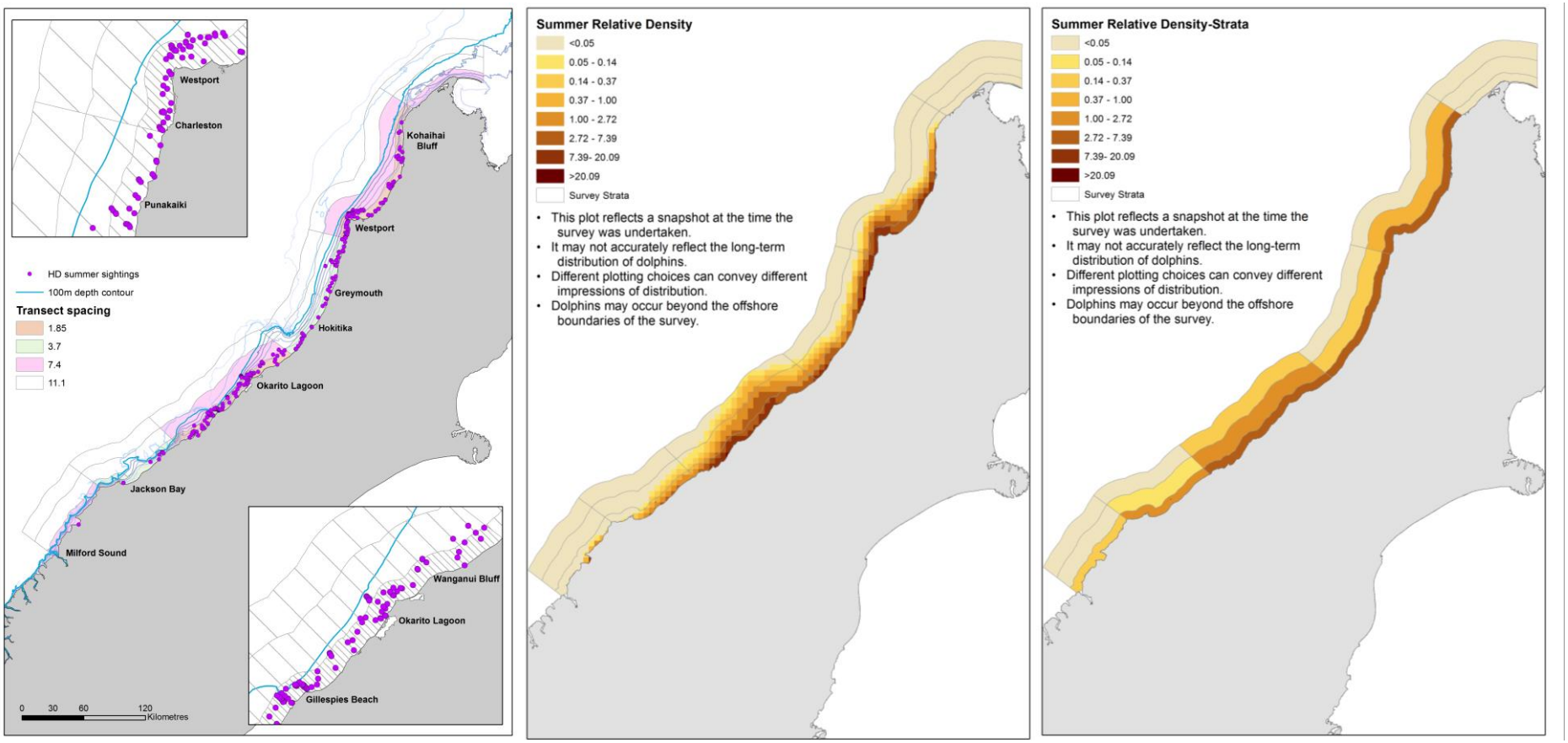

Figure 15a: Hector's dolphin summer distribution assessed from aerial line-transect surveys. Panels represent patterns for all on-effort Hector's dolphin sightings (left), the relative density of Hector's dolphins within 5 km × 5 km grid cells generated from the Density Surface Models with eight categories (middle) and the relative density of Hector's dolphins within survey strata generated from the Density Surface Models (right). Relative densities greater than 1 indicate areas with density greater than the overall average density.

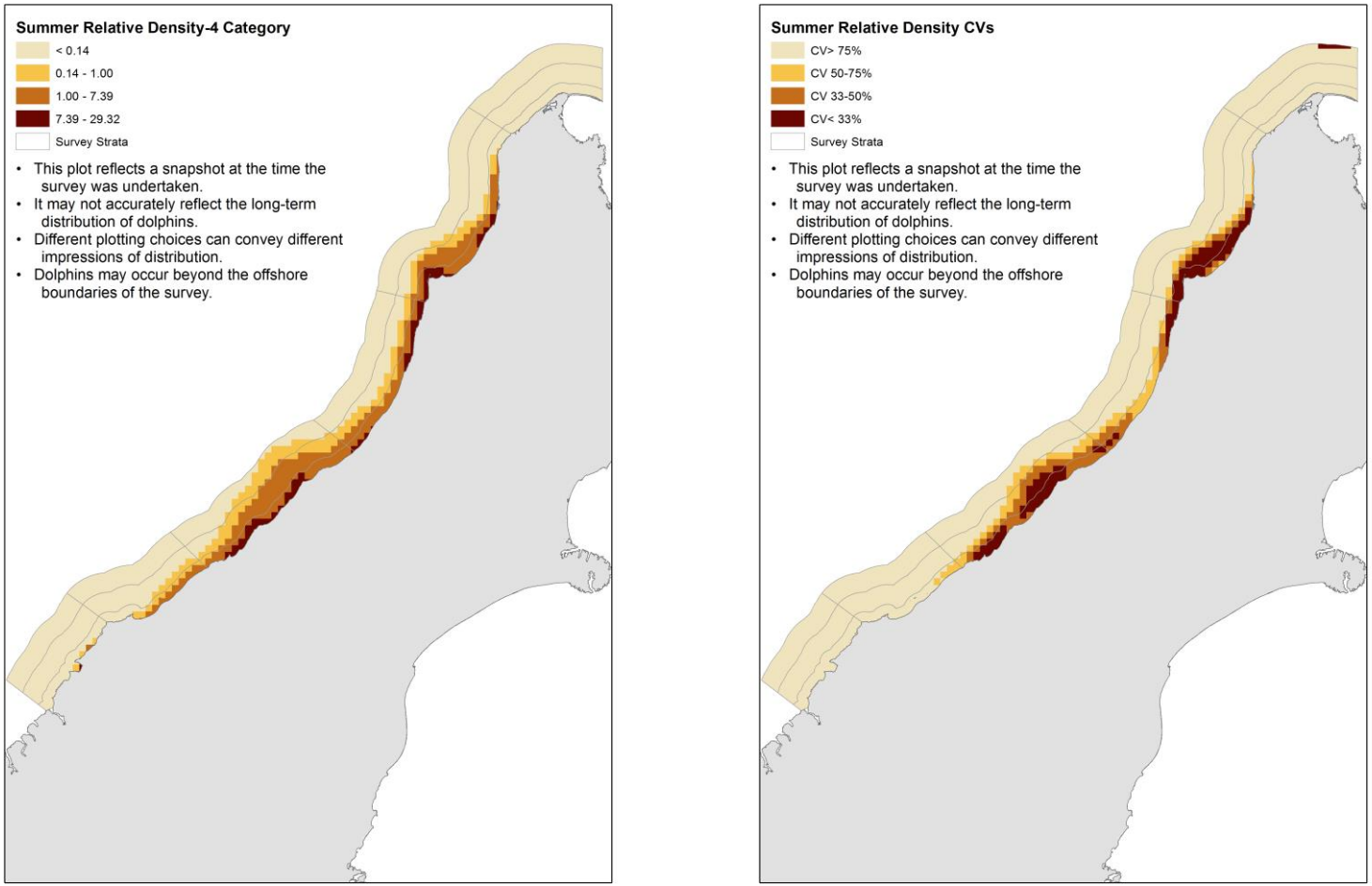

Figure 15b: Hector's dolphins summer distribution assessed from aerial line-transect surveys. Panels represent the relative density of Hector's dolphins within 5 km × 5 km grid cells generated from the Density Surface Model with four density categories (left), and the precision of estimated relative density with darker colours indicating greater precision; i.e. smaller CVs (right). Relative densities greater than 1 indicate areas with density greater than the overall average density.

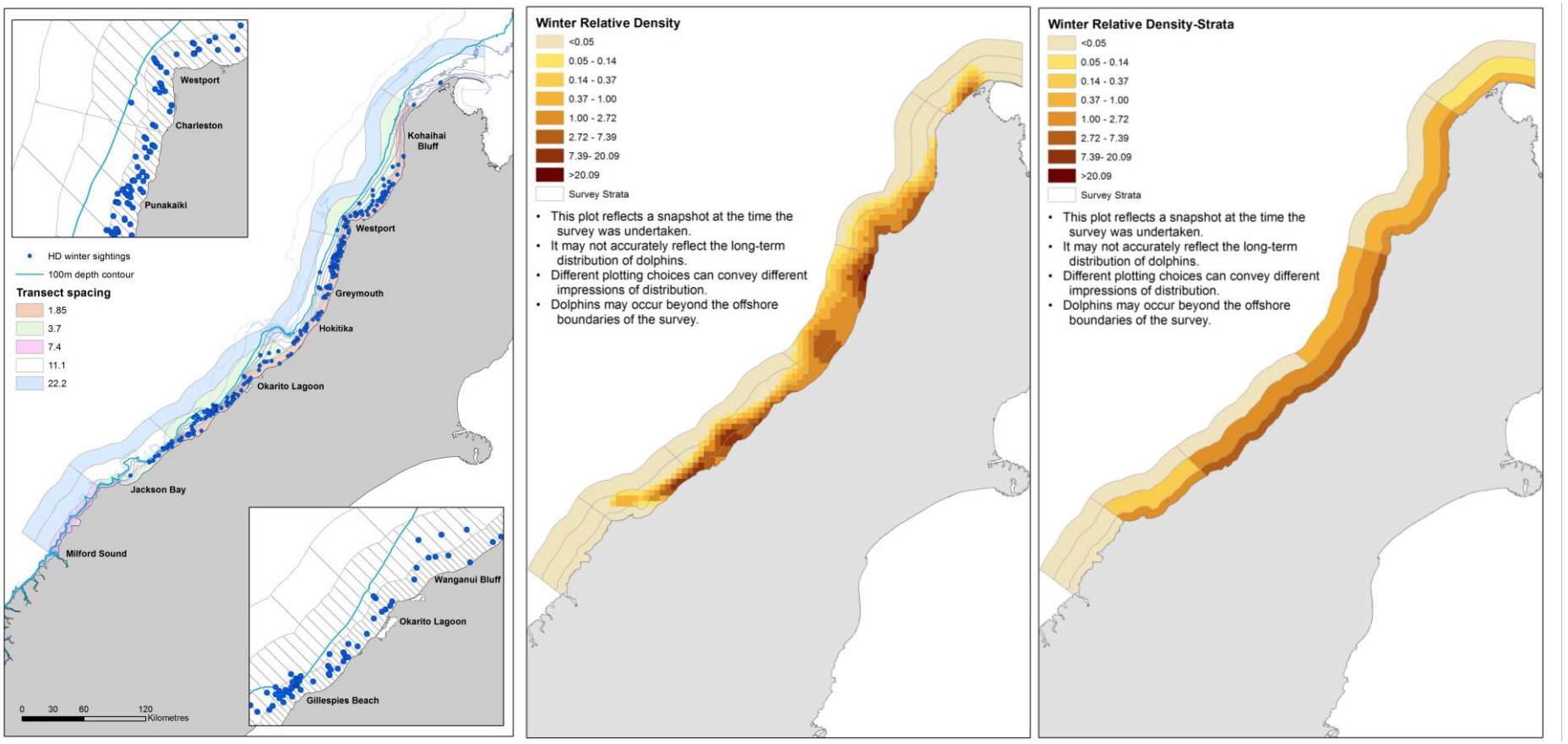

Figure 16a: Hector's dolphin winter distribution assessed from aerial line-transect surveys. Panels represent patterns for all on-effort Hector's dolphin sightings (left), the relative density of Hector's dolphins within 5 km × 5 km grid cells generated from the Density Surface Models with eight categories (middle) and the relative density of Hector's dolphins within survey strata generated from the Density Surface Models (right). Relative densities greater than 1 indicate areas with density greater than the overall average density.

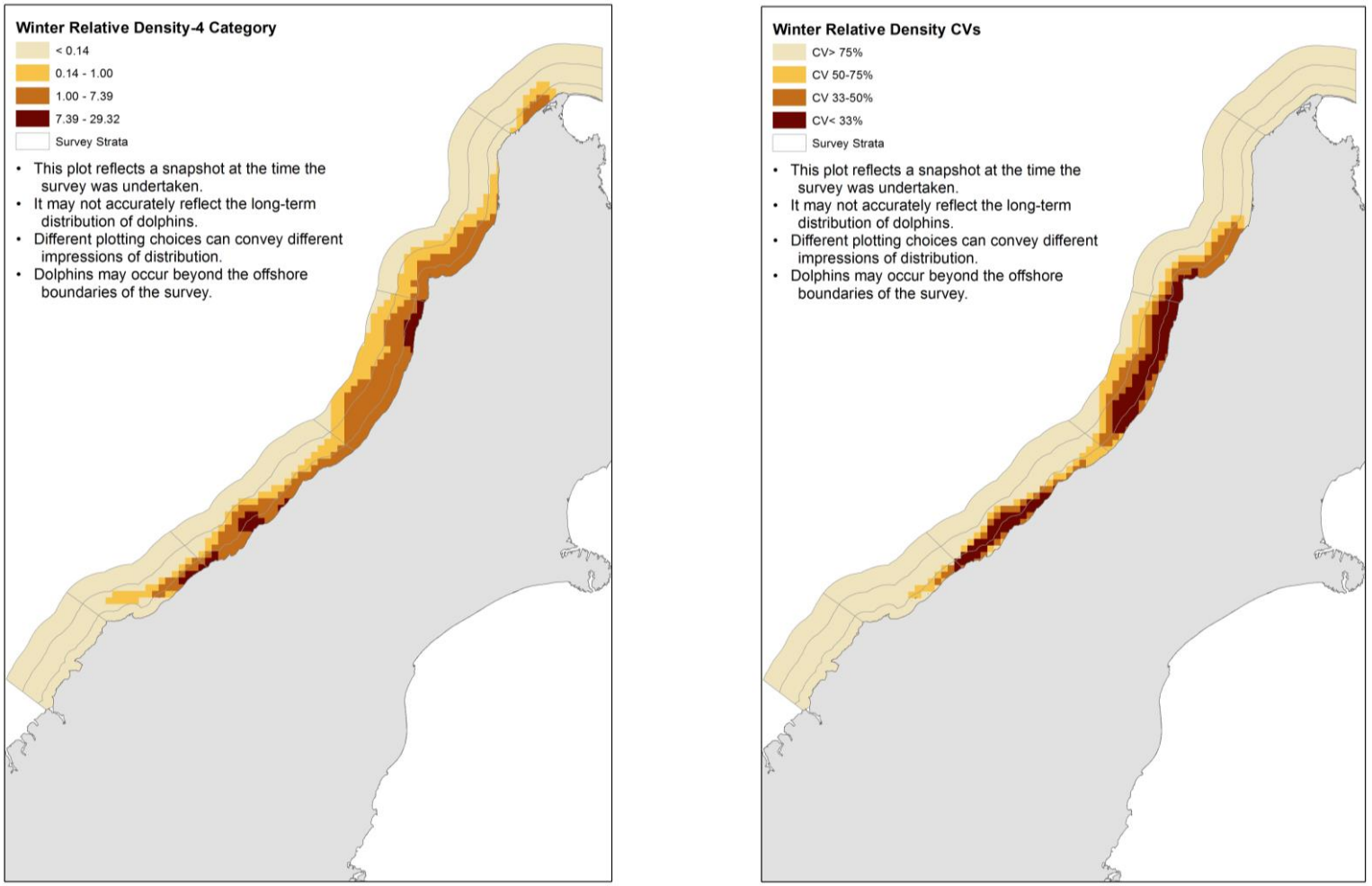

Figure 16b: Hector's dolphins winter distribution assessed from aerial line-transect surveys. Panels represent the relative density of Hector's dolphins within 5 km × 5 km grid cells generated from the Density Surface Model with four density categories (left), and the precision of estimated relative density with darker colours indicating greater precision; i.e. smaller CVs (right). Relative densities greater than 1 indicate areas with density greater than the overall average density.

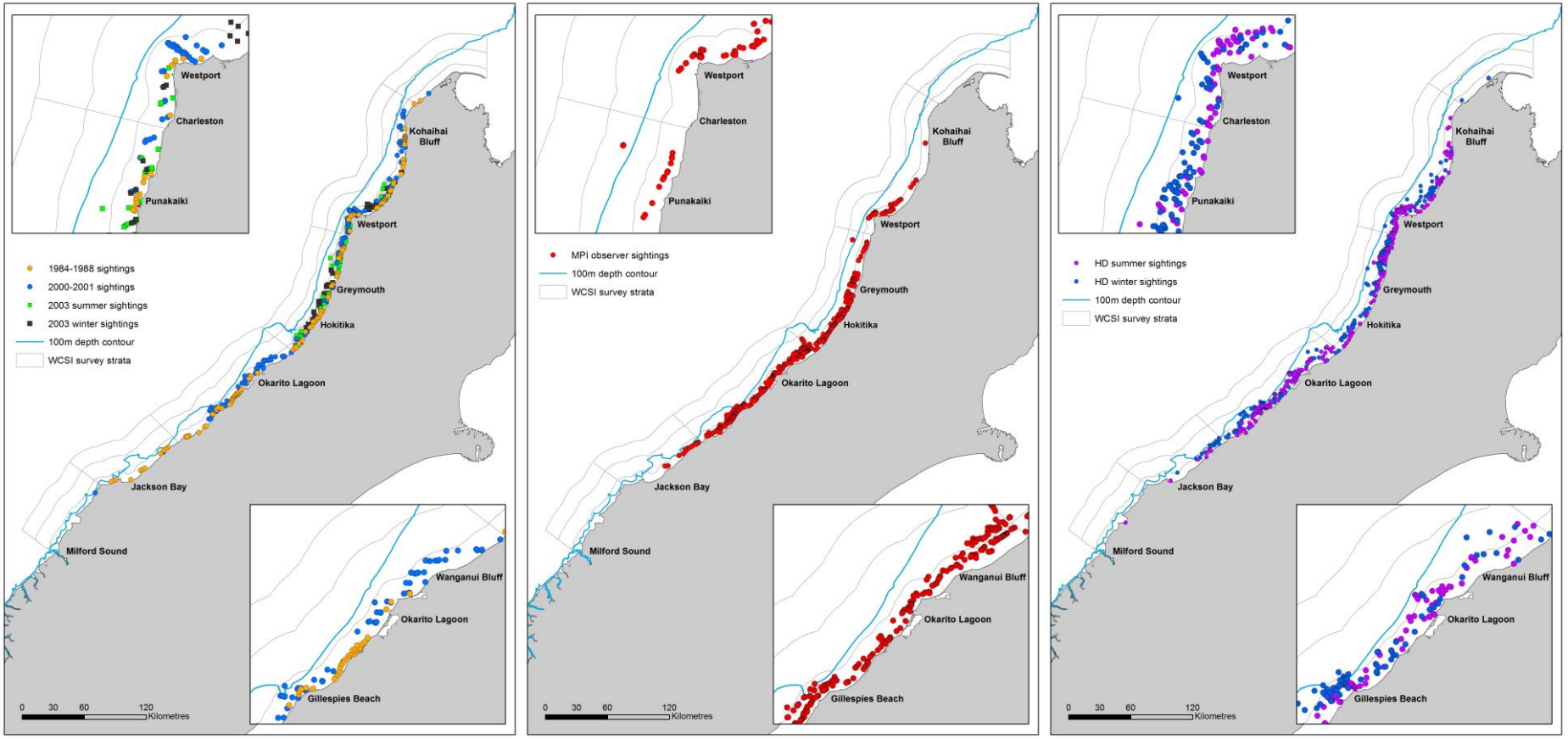

Figure 17: Locations of Hector's dolphin sightings along the WCSI from previous boat- and aerial-based surveys (left), Ministry for Primary Industries observers (centre) and present surveys (right).

The results of the summer and winter DSMs are given in Figure 15–16. The right-hand panels of Figure 15band 16b indicate the precision of the relative abundance estimates from the DSM and tend to be greatest in those areas with higher relative density. Estimated summer and winter dolphin density (per 100 km^2) for each stratum are given in Table 28 and Table 29 lists the group-size frequencies used in the parametric bootstrap for each season.

Standard errors were obtained using 510 bootstrap data sets. This is a sufficient number for approximating standard errors (Manly 1997). Valid standard errors for the detection function were not obtained for 14 bootstrap datasets for the summer analysis, and for 22 bootstrap datasets for the winter analysis. Eight bootstrap data sets for the winter analysis also produced estimates of total dolphin abundance that were greater than 15 000 dolphins, which was considered extreme. Therefore, standard errors for the summer DSM were determined from 496 bootstrap samples and 480 bootstrap samples for the winter DSM.

Total abundance was estimated from the DSM as 6497 (SE = 852) for the summer and 7068 (SE = 1377) during the winter. The summer value is in very good agreement with the non-DSM abundance estimate using the top-ranked detection function model and the helicopter-based estimates of availability (6379, SE = 1057, Table SM.Q.1), although the winter value is notably higher than the corresponding non-DSM estimate (5937, SE = 822, Table SM.R.1).

The relative precision (i.e., the CV) of DSM-based stratum-specific estimates tended to be at least as good as the non-DSM estimates, particularly for those strata with non-negligible estimates (although not in all instances; Table 30). While the CVs presented in Table 30 are for density estimates, the same CVs would hold for stratum-specific abundance estimates. A direct comparison is slightly impeded by the estimates from the two different approaches being somewhat different for some strata, which is primarily a result of the smooth density surface created by the GAM.

Table 28: Estimated summer and winter density (Density; per 100km^2) for each strata from DSM analysis using top-ranked detection model in Tables 5 and 9, and dive-cycle based availability estimates. Standard errors (SE) obtained from a parametric bootstrap approach with 504 bootstrapped data sets for summer and 477 for winter.

		Summer		Winter	
Coastal Section	**Offshore Stratum (nmi)**	**Density**	**SE**	**Density**	**SE**
Whanganui Inlet	0–4			19	29
	4–12			2	3
	12–20			0	27
Hector	0–4	124	16	60	16
	4–12	16	5	15	6
	12–20			1	1
Greymouth	0–4	152	36	160	37
	4–12	9	5	68	20
	12–20			13	9
Okarito Lagoon	0–4	162	38	136	29
	4–12	38	12	32	10
	12–20	4	3	0	1
Jackson Bay	0–4	27	14	63	25
	4–12	1	2	8	7
	12–20				
Milford Sound	0–4	6	10		
	4–12				
	12–20				
Overall		**25**	**3**	**27**	**5**

Table 29: Group-size frequency table used to randomly generate group sizes in the parametric bootstrap procedure. Results presented are the number of observed groups of size *s* (n_s), the expected probability of detecting a group of size *s* within the covered area ($E(p_\bullet(s))$), and is the estimated frequency of group size *s* ($\hat{f}_s$). The estimated number of groups in the covered area ($\hat{N}_{gc}$) was 346.44 in summer and 402.24 in winter.

	Summer			Winter		
Size	n_s	$E(p_\bullet(s))$	$\hat{f}_s$	n_s	$E(p_\bullet(s))$	$\hat{f}_s$
1	174	0.64	0.50	221	0.61	0.55
2	98	0.74	0.28	111	0.70	0.28
3	42	0.83	0.12	43	0.79	0.11
4	21	0.90	0.06	19	0.86	0.05
5	1	0.94	0.00	2	0.91	0.01
6	4	0.97	0.01	4	0.95	0.01
7	4	0.99	0.01			
8	1	0.99	0.00			
9	1	1.00	0.00			
11				1	1.00	0.00
16				1	1.00	0.00

Table 30: Comparison of DSM-based estimates of dolphin density (per 100 km^2) each season with those obtained from the corresponding non-DSM analyses (top-ranked models in SM Table J.1 and L.1 appendices).

		Summer				Winter			
Coastal Section	**Offshore Stratum (nmi)**	**non-DSM**	**CV**	**DSM**	**CV**	**non-DSM**	**CV**	**DSM**	**CV**
Whanganui Inlet	0–4					27	75%	19	156%
	4–12							2	168%
	12–20								
Hector	0–4	117	21%	124	13%	61	22%	60	26%
	4–12	22	73%	16	31%	10	30%	15	42%
	12–20							1	138%
Greymouth	0–4	150	23%	152	23%	171	23%	160	23%
	4–12	3	92%	9	55%	26	57%	68	30%
	12–20							13	71%
Okarito Lagoon	0–4	164	24%	162	23%	139	20%	136	21%
	4–12	37	75%	38	31%	24	35%	32	30%
	12–20			4	79%				
Jackson Bay	0–4	32	59%	27	55%	82	44%	63	40%
	4–12			1	178%			8	91%
	12–20								
Milford Sound	0–4	5	75%	6	152%				
	4–12								
	12–20								
Overall		**24**	**17%**	**25**	**13%**	**23**	**14%**	**27**	**19%**

3.3 South Island Abundance and Distribution Estimate

SI Abundance

Detailed information on the summary sighting data, the detection function reanalysis and availability bias for the SCSI are provided in SM Section S. The reanalysed estimates of dolphin abundance for SCSI, after correcting for detection, detection function model uncertainty and availability bias are 177 for March (CV: 37%; 95% CI: 88–358) and 299 for August (CV: 47%; 95% CI: 125–714). The average estimate is 238 (CV: 40%; 95% CI: 113–503). This estimate is notably lower than that obtained by Clement et al. (2011), which is largely due to higher availability estimates in the reanalysis when allowing for the length of time a dolphin group remains in the field of view of an observer. See SM Section S for further discussion.

A reanalysis of the ECSI survey data using the same methods as those employed for the WCSI survey data yields a summer abundance estimate of 9728 (CV: 17%; 95% CI: 7001–13 517) and 8208 (CV 27%; 95% CI: 4888–13 785) in winter. The average abundance estimate for ECSI is 8968 (CV: 15%; 95% CI: 6649–12 096). Details of the reanalysis results are given in Section T of the SM.

A summary of the abundance estimates for each region are given in Table 31, resulting in a total abundance estimate for Hector's dolphin around the South Island of 14 849 (CV: 11%; 95% CI: 11 923–18 492).

Table 31: South Island abundance estimate of Hector's dolphin calculated from surveys conducted in south coast South Island (SCSI; surveyed 2010), east coast South Island (ECSI; surveyed 2013) and west coast South Island (WCSI; surveyed 2015). Standard errors are in parentheses.

	Summer	Winter	Average
SCSI	177 (66)	299 (140)	238 (94)
ECSI	9 728 (1 644)	8 208 (2 210)	8 968 (1 377)
WCSI	5 482 (1 433)	5 802 (1 205)	5 642 (936)
South Island			**14 849** **(1 668)**

SI Distribution

The relative densities from the DSM from each survey region were scaled to be comparable to one another by multiplying by the regional density and dividing by the overall SI density (Figure 18-19). The average values from Table 31 were used to make this adjustment. Therefore, a value of 1 in Figure 19 indicates a cell with density equal to the SI-wide average.

The greatest densities of Hector's dolphins were located along the middle sections of both the east and west coastlines (between latitude S41º30´ and S44º) and the Clifford/Cloudy Bay region (Figure 18–19). Only small, localised densities of dolphins were observed along north-western and southern coastal regions. We stress that the estimated distribution indicated in Figure 19 is based on the location of the sighted dolphin groups at the exact time of the surveys (Figure 18). It is unknown how representative this might be of where dolphins are likely to be generally, and the degree of temporal variation at daily, seasonal and annual timescales.

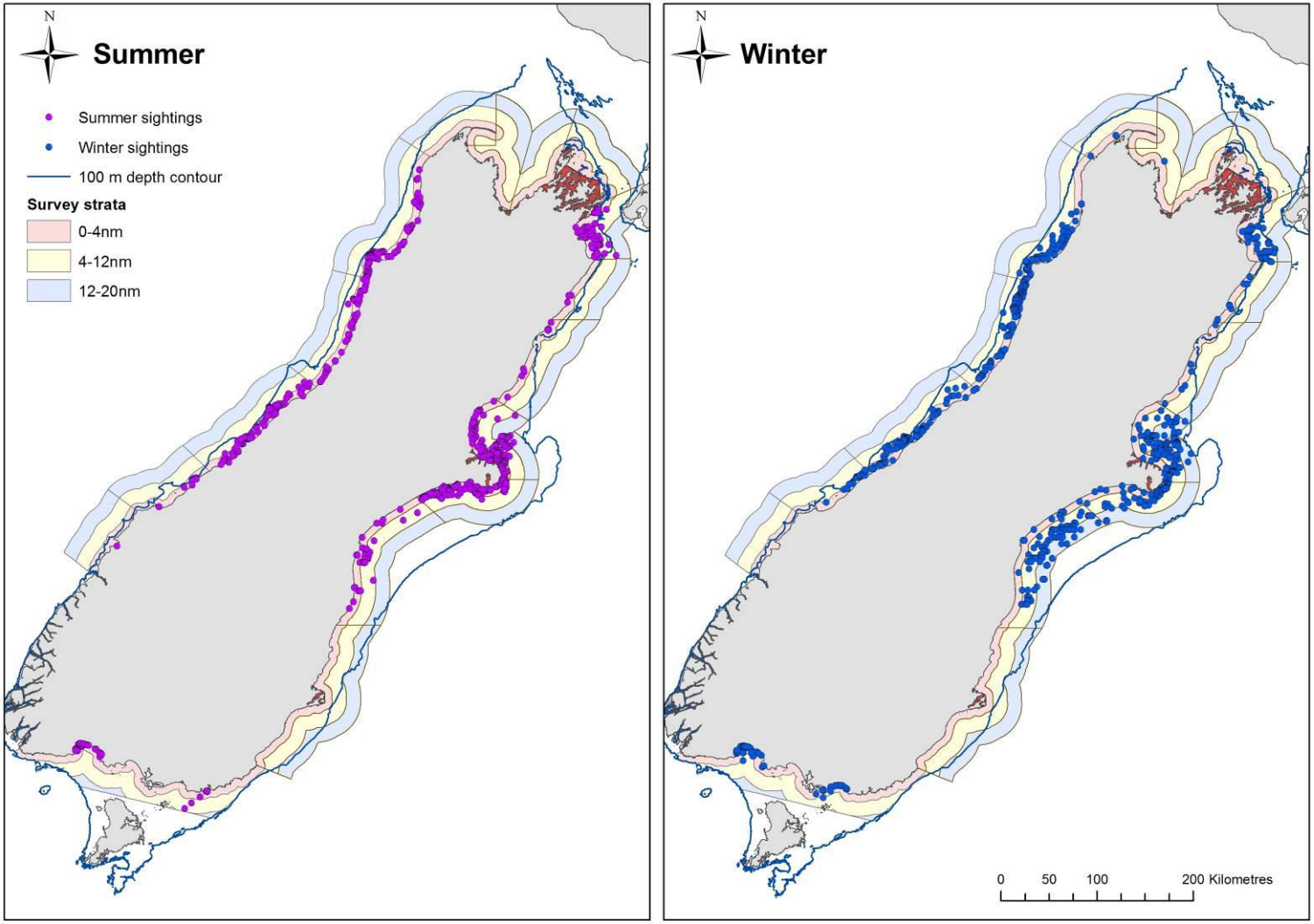

Figure 18: Hector's dolphin summer (left) and winter (right) sightings from the three separate abundance surveys: east coast (WCSI) completed 2015, east and north coast (ECSI) completed in 2013 and south coast (SCSI) completed in 2010.

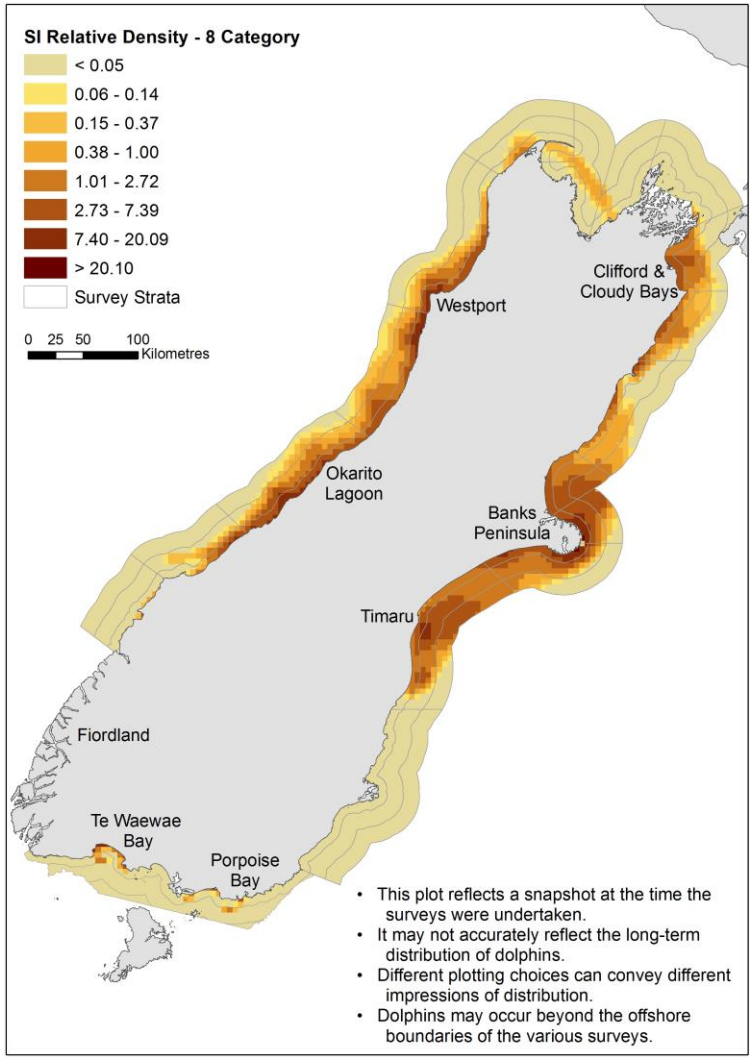

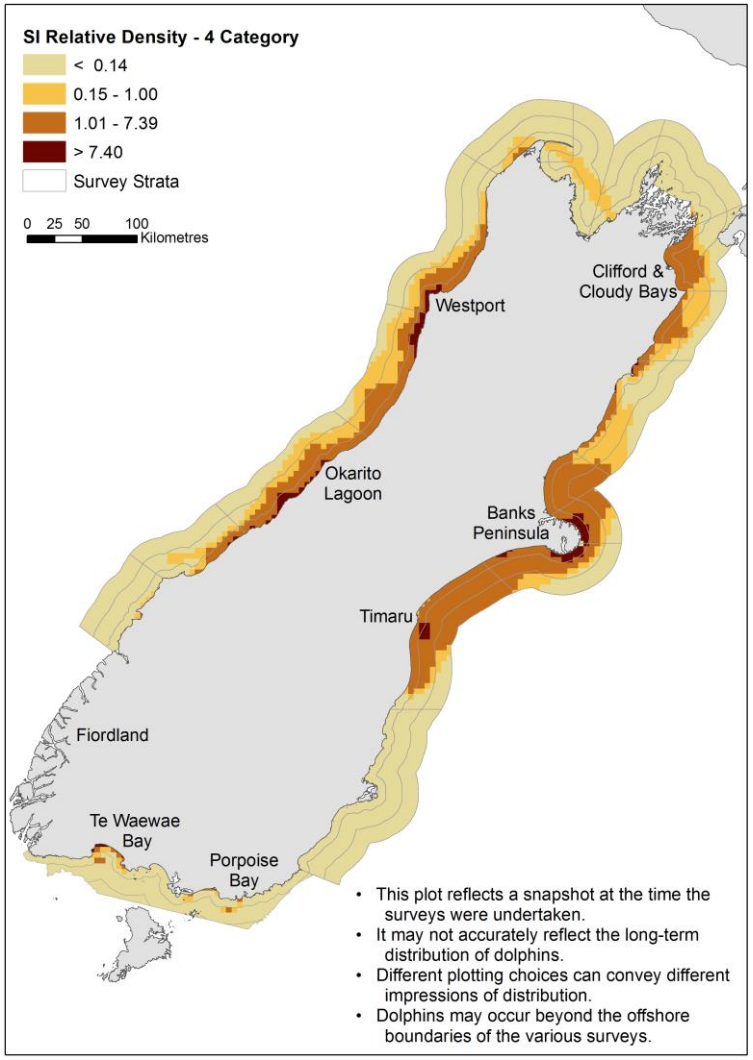

Figure 19a: The South Island distribution of Hector's dolphin assessed from both summer and winter aerial line-transect surveys. Panels represent patterns for the relative density of Hector's dolphins within 5 km × 5 km grid cells generated from the Density Surface Models with eight categories (left) and the relative density of Hector's dolphins within survey strata generated from the Density Surface Models (right). Relative densities greater than 1 indicate areas with density greater than the overall average density.

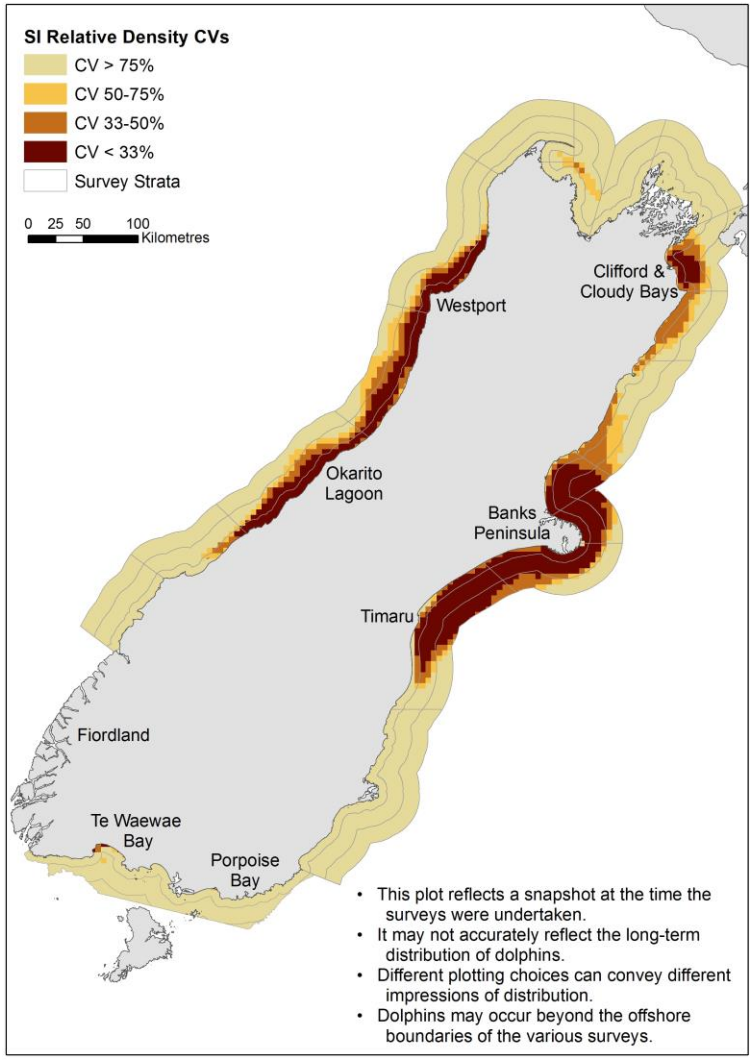

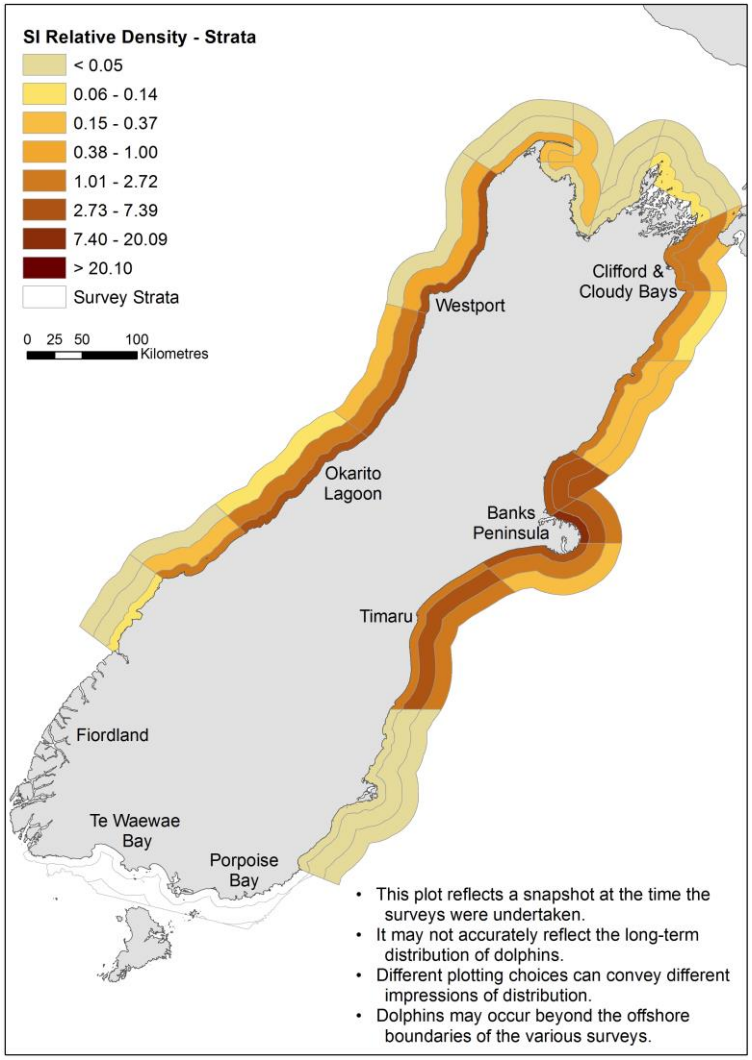

Figure 19b: The South Island distribution of Hector's dolphin assessed from both summer and winter aerial line-transect surveys. Panels represent patterns for the precision of estimated relative density with darker colours indicating greater precision; i.e. smaller CVs (left) and the relative density of Hector's dolphins within survey strata generated from the Density Surface Models (right). Relative densities greater than 1 indicate areas with density greater than the overall average density.

4. DISCUSSION

4.1 WCSI abundance and distribution

Slooten et al. (2004) estimated Hector's dolphin abundance within four nmi of the WCSI coastline as 5388 (95% CI: 3613–8034) from aerial surveys conducted during the summer of 2000/01. This is in good agreement with our current seasonal WCSI estimates (summer: 5490, 95% CI 3319–9079; winter: 5802, 95% CI 3879–8679). However one point of difference is that Slooten et al. (2004) did not record any dolphin sightings in their offshore stratum (4–10 nmi), while we had 16 groups sighted in summer beyond four nmi and 29 in winter (from the full datasets). Correcting for this difference, approximate 4285 dolphins in summer and 4560 dolphins in winter were estimated within the 0–4 nmi, still well within the 95% confidence intervals of the 2000/2001 estimate. Slooten et al. (2004) survey effort in the 4–10 nmi stratum was an order of magnitude lower than in our 4–12 nmi strata effort, suggesting that the lack of sightings in 2000/2001 may have just been an unfortunate consequence of low effort. It may also be due to inter-annual variation in dolphin distribution due to differences in oceanic conditions, prey distribution, etc.

The alongshore distribution of dolphin density largely matched with our *a priori* expectations; based on distribution patterns from previous Hector's dolphin aerial survey work (i.e., Slooten et al. 2004, Rayment et al. 2010b). The exception being a greater number of dolphins are currently estimated to be in the GREY stratum, and in offshore areas. Greater densities of dolphins were found closer to shore between Hector and Punakaiki to the north and off Okarito Lagoon and Bruce Bay in the south over the summer months. During winter, high density areas occurred mainly off Punakaiki and in the vicinity of the deep water canyons off Gillespie Beach. These regions generally match previous patterns found in seasonal surveys by Rayment et al. (2010).

Current fisheries protective measures off the west coast of the South Island include a year-round ban on recreational set net fishing from Farewell Spit to Awarua Point (north of Fiordland) and offshore to two nmi. Commercial set netting is banned in the same region from 1 December to 28 February (i.e. summer months). Prior to the introduction of these set net restrictions in 2008, an estimated 70–100 Hector's dolphins per year were predicted to be caught as commercial bycatch (Davies et al. 2008) and the west coast sub-population was projected to be declining (Slooten 2007, Davies et al. 2008). It is probably too early and there is too little data to robustly assess whether current fisheries restrictions measures are having an impact on population growth; although, the current WCSI Hector's dolphin population estimates suggest that no extreme changes (positive or negative) have occurred since the previous abundance survey approximately 15 years ago.

4.2 South Island abundance and distribution

Our estimate of Hector's dolphin abundance around the South Island is 14 849 (95% CI: 11 923–18 492), which is approximately twice as large as the previous estimate of 7300 animals (95% 5303–9966; Slooten et al. 2004). This difference is primarily due to our much higher estimate of the population size along the ECSI. In comparison with the previous estimate, however, it is important to realise that the present survey encompassed a much larger area, including previously unsurveyed offshore areas that were estimated to contain

dolphins in substantial numbers (i.e., approximately 50% of the ECSI population was estimated to be beyond four nmi).

Our surveys also found fairly similar densities of Hector's dolphin occurring along parts of both the east and west coastal regions; contrary to the previous survey findings (Slooten et al. 2004) in which the west coast population was considered the major stronghold for this species. However, smaller densities of Hector's dolphins in north-western and southern coastal areas still represent localised and potentially isolated remnant sub-populations.

That Hector's dolphin are more abundant and likely to be found in offshore areas that have been previously unidentified has important ramifications for the conservation management of this species; particular in context of current Threat Management Plan review and on our understanding of the likely impact of fishing activities on the population (e.g., Davies et al. 2008, Slooten & Dawson 2010, Slooten & Davies 2012).

5. ACKNOWLEDGMENTS

Work for Objectives 1–5 was completed for the Ministry for Primary Industries (MPI) under contract PRO2013-06. Additional data used to complete Objective 6 was collected under MPI contracts PRO2009-01A, PRO2009-01B and PRO2009-01C.

This work would never have been completed without the enduring patience and superb search image of the survey teams that helped throughout various stages of the field work. In particular, we need to thank Christina McClay for leading several of the teams and helping to process data.

We would also like to thank all the supporting organisations and people that assisted in the field work portion of this project including: Flight Hauraki (Paul McSherry and William Hayman), the Garden City Helicopter (and former Helipro) staff in Christchurch and Wellington (in particular Regan Graham), Department of Conservation Golden Bay, Te Anau and Hokitika offices, Jenny Ladley and the University of Canterbury's Maxwell Gage field station in Westport, Blue Water Survival Training Specialists, the Omaka Aero club, and the Knightsbridge Court Motel in Blenheim. Thanks also to Rachel Fewster, Rob Mattlin, Steve Buckland, Jeff Laake and Phil Hammond who have scrutinised various versions of this and related reports.

6. REFERENCES

Anderson, D.R. (2008). Model based inference in the life sciences. Springer. New York, USA.

Baker, C.S.; Chilvers, B.L.; Constantine, R.; DuFresne, S.; Mattlin, R.H.; van Helden, A.; Hitchmough, R. (2010). Conservation status of New Zealand marine mammals (suborders Cetacea and Pinnipedia), 2009. *New Zealand Journal of Marine and Freshwater Research, 44(2)*: 101 – 115.

Borchers, D.L.; Laake, J.L.; Southwell, C.; Paxton, C.G.M. (2006). Accommodating unmodeled heterogeneity in double-observer distance sampling surveys. *Biometrics* 62, 372–378.

Buckland, S.T.; Anderson, D.R.; Burnham, K.P.; Laake, J.L.; Borchers, D.L.; Thomas, L. (2001). Introduction to Distance Sampling: Estimating abundance of biological populations. Oxford University Press, New York.

Buckland, S.T.; Anderson, D.R.; Burnham, K.P.; Laake, J.L.; Borchers, D.L.; Thomas, L. (2004). Advanced Distance Sampling: Estimating abundance of biological populations. Oxford University Press, New York.

Buckland, S.T.; Laake, J.L.; Borchers, D.L. (2010). Double-observer line transect methods: levels of independence. *Biometrics* 66: 169–177.

Burnham, K.P.; Anderson, D.R. (2002). Model selection and multimodel inference. 2nd Ed., Springer-Verlag, New York, USA.

Clement, D.; Mattlin, R.; Torres, L. (2011). Abundance, distribution and productivity of Hector's (and Maui's) dolphins Final Research Report, PRO2009-01A. (Unpublished report held by Ministry for Primary Industries, Wellington.)

Davies, N.M.; Brian, R.; Starr, P.; Lallemand P.; Gilbert, D.; McKenzie, J. (2008). Risk analysis for Hector's dolphin and Maui's dolphin subpopulations to commercial set net fishing using a temporal-spatial age-structured model. (Final Research Report held by Ministry for Primary Industries.)

Dawson, S.; Slooten, E. (1988). Hector's Dolphin *Cephalorhynchus hectori*: Distribution and abundance. *Reports International Whaling Commission Special issue 9*: 315–324.

Dawson, S.; Slooten, E.; Du Fresne, S.; Wade, P.; Clement, D. (2004). Small-boat surveys for coastal dolphins: line-transect surveys for Hector's dolphin (*Cephalorhynchus hectori*). *Fishery Bulletin* 102(3): 441–451.

Dawson, S.; Wade, P.; Slooten, E.; Barlow, J. (2008). Design and field methods for sighting surveys of cetaceans in coastal and riverine habitats. *Mammal Review* 38(1): 19–49.

Department of Conservation, Ministry of Fisheries (2007). Hector's and Maui's dolphin threat management plan draft for public consultation. 5 March 2009.http://www.fish.govt.nz/NR/rdonlyres/2088EFD2008C-E2207-4798-9315-C2000AF2002FC2006FFB2002/2000/DRAFTTMPFINAL.pdf

DuFresne, S.; Mattlin, R. (2009). Distribution and Abundance of Hector's Dolphin (Cephalorhynchus hectori) in Clifford and Cloudy Bays (Final report for NIWA project CBF07401). Marine Wildlife Research Ltd.

DuFresne, S.; Mattlin, R.; Clement, D. (2010). Distribution and Abundance of Hector's Dolphin (*Cephalorhynchus hectori hectori*) and Observations of Other Cetaceans in Pegasus Bay. Final Report to the Marlborough Mussel Company, Baseline Monitoring for Environment Canterbury Consent CRC21013A.

Gomez-de-Segura, A.; Hammond, P.S.; Canadas, A.; Raga J.A. (2007). Comparing cetacean abundance estimates derived from spatial models and design-based line transect methods. *Marine Ecology Progress Series* 329: 289–299.

Hamner, R.M.; Oremus, M.; Stanley, M.; Brown, P.; Constantine, R.; Baker, C.S. (2012). Estimating the abundance and effective population size of Maui's dolphins using microsatellite genotypes in 2010–11, with retrospective matching to 2001–07. Department of Conservation, Auckland. 44 p.

Hiby, L. (1999). The objective identification of duplicate sightings in aerial survey for porpoise, in Marine Mammal Survey and Assessment Methods, eds Garner, G.W. Amstrup, S.C.; Laake, J.L.; Manly, B.F.J.; McDonald, L.L.; Robertson, D.G. Balkema, Rotterdam, pp. 179–189.

Laake, J.L.; Borchers, D.L. (2004). Methods for incomplete detection at distance zero. Pp. 108–189 in *Advanced Distance Sampling*, eds Buckland, S.T.; Anderson, D.R.; Burnham, K.P.; Laake, J.L.; Borchers, D.L.; Thomas, L. Oxford University Press, Oxford.

MacKenzie, D.I.; Clement, D.; Mattlin, R. (2012). Abundance, distribution and productivity of Hector's (and Maui's) dolphins (Final Research Report, PRO2009-01B). (Unpublished report held by the Ministry for Primary Industries.)

MacKenzie, D.I.; Clement, D.M. (2014). Abundance and distribution of ECSI Hector's dolphin. *New Zealand Aquatic Environment and Biodiversity Report No. 123*. 79 p.

MacKenzie, D.I.; Clement, D.M. (2016). Accounting for Lack of Independence and Partial Overlap of Observation Zones in Line-Transect Mark-recapture Distance Sampling. *Journal of Agricultural, Biological, and Environmental Statistics 21:* 41–57. DOI 10.1007/s13253-015-0234-1.

Manly, B.F.J. (1997). Randomization, bootstrap and Monte Carlo methods in biology. 2nd edition. Chapman and Hall, London, U.K.

Manly, B.F.J.; McDonald, L.L.; Garner. G.W. (1996). Maximum likelihood estimation for the double-count method with independent observers. *Journal of Agricultural and Biological Statistics 1*: 170–189.

Pichler, F.B.; Dawson, S.M.; Slooten, E.; Baker, C.S. (1998). Geographic isolation of Hector's dolphin populations described by mito-chondrial DNA sequences. *Conservation Biology 12*:676–682.

Rayment, W.; Dawson, S.; Slooten, E. (2010a). Seasonal changes in distribution of Hector's dolphin at Banks Peninsula, New Zealand: implications for protected area design. *Aquatic Conservation: Marine and Freshwater Ecosystems 20*: 106–116.

Rayment, W.; Clement, D.; Dawson, S.; Slooten, E.; Secchi, E. (2010b). Distribution of Hector's dolphin (*Cephalorhynchus hectori*) off the west coast, South Island, New Zealand, with implications for the management of bycatch. *Marine Mammal Science 27*: 398−420

Reeves, R.R.; Dawson, S.M.; Jefferson, T.A.; Karczmarski, L.; Laidre, K.; O'Corry-Crowe, G.; Rojas-Bracho, L.; Secchi, E.R.; Slooten, E.; Smith, B.D.; Wang, J.Y.; Zhou, K. (2008). *Cephalorhynchus hectori maui*. In: IUCN 2011. IUCN Red List of Threatened Species. Version 2011.1.http://www.iucnredlist.org

Slooten, E. (2007). Conservation management in the face of uncertainity: effectiveness of four options for managing Hector's dolphin bycatch. *Endangered Species Research* (3): 169–179.

Slooten, E.; Davies, N.M. (2012). Hector's dolphin risk assessments: old and new analyses show consistent results. *Journal of the Royal Society of New Zealand 42*: 49–60.

Slooten, E.; Dawson, S.M. (2010). Assessing the effectiveness of conservation management decisions: Likely effects of new protection measures for Hector's dolphin. *Aquatic Conservation: Marine and Freshwater Ecosystems 20*: 334–347.

Slooten, E.; Dawson, S.; Rayment, W. (2004). Aerial surveys for Hector's dolphins: abundance of Hector's dolphins off the South Island west coast, New Zealand. *Marine Mammal Science* 20, 477–490.

Slooten, E.; Dawson, S.; Rayment, W.; Childerhouse, S. (2006). A new abundance estimate for Maui's dolphin: What does it mean for managing this critically endangered species. *Biological Conservation* 128 (4): 576-581.